(1)

THE OHIO STATE UNIVERSITY

JOINT SERVICES ELECTRONICS PROGRAM

Twelfth Annual Report

The Ohio State University

ElectroScience Laboratory

Department of Electrical Engineering
Columbus, Ohio 43212

Annual Report 721563-1
Contract No. N00014-89-K-1007
November 1989

Department of the Navy
Office of Naval Research
800 North Quincy Street
Arlington, Virginia 22217

NOTICES

When Government drawings, specifications, or other data are used for any purpose other than in connection with a definitely related Government procurement operation, the United States Government thereby incurs no responsibility nor any obligation whatsoever, and the fact that the Government may have formulated, furnished, or in any way supplied the said drawings, specifications, or other data, is not to be regarded by implication or otherwise as in any manner licensing the holder or any other person or corporation, or conveying any rights or permission to manufacture, use, or sell any patented invention that may in any way be related thereto.

50272-101

REPORT DOCUMENTATION PAGE	1. REPORT NO.	2.	3. Recipient's Accession No.
4. Title and Subtitle Joint Services Electronics Program – Twelfth Annual Report			5. Report Date November 1989 6.
7. Author(s) Leon Peters, Jr.			8. Performing Org. Rept. No. 721563-1
9. Performing Organization Name and Address The Ohio State University ElectroScience Laboratory 1320 Kinnear Road Columbus, OH 43212			10. Project/Task/Work Unit No. 11. Contract(C) or Grant(G) No. (C) N00014-89-K-1007 (G)
12. Sponsoring Organization Name and Address Department of the Navy, Office of Naval Research 800 North Quincy Street Arlington, Virginia 22217			13. Report Type/Period Covered Annual Report 14.
15. Supplementary Notes			
16. Abstract (Limit: 200 words)			
17. Document Analysis a. Descriptors b. Identifiers/Open-Ended Terms c. COSATI Field/Group			
18. Availability Statement A. Approved for public release; Distribution is unlimited.	19. Security Class (This Report) Unclassified 20. Security Class (This Page) Unclassified		21. No. of Pages 80 22. Price

(See ANSI-Z39.18) *See Instructions on Reverse* OPTIONAL FORM 272 (4-77)
Department of Commerce

Contents

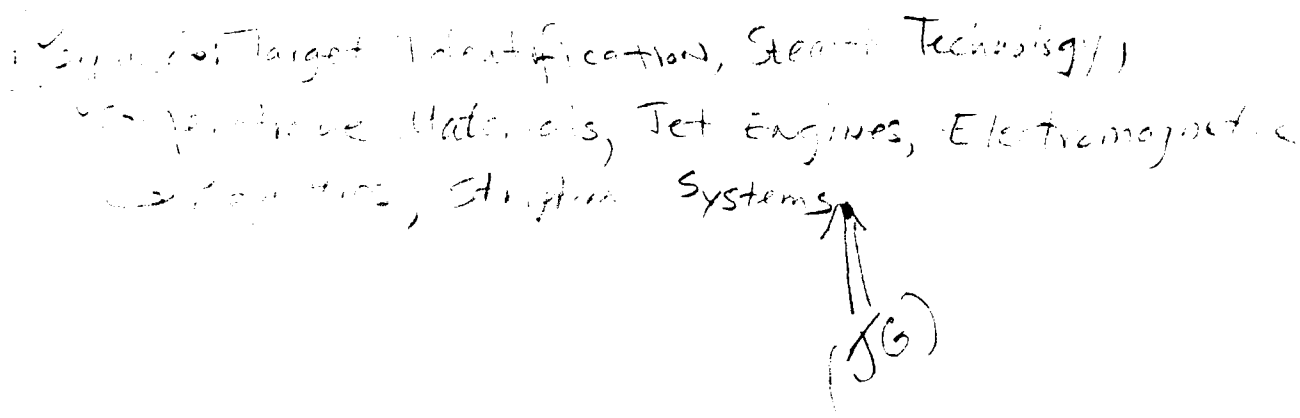

List of Figures

I. DIRECTORS OVERVIEW

This report represents the twelfth annual summary of The Ohio State University Joint Services Program (JSEP).

There have been a total 25 Ph.D. and 19 M.Sc degrees in Electrical Engineering obtained under partial JSEP sponsorship. There are currently 8 Ph.D. and 3 M.Sc. students being partially supported under JSEP.

As may be seen in the Annual report Appendix, 18 reprints have been included in the period September 1988 to September 1989. In addition, 10 papers have already been accepted for publication in the coming year, an additional 11 papers have been submitted, and an additional 15 papers are in preparation.

II. DESCRIPTION OF SPECIAL ACCOMPLISHMENTS AND TECHNOLOGY TRANSITION

The transfer of the compact range and target identification technology initiated under JSEP support for time domain studies continues to make large advances. Using other sources of support design for a mini chamber has now been generated and is being constructed.

The research has proven to be of intense interest to DoD and the Aerospace industry and we have now added three new members to our Compact Range Consortium. There are now 16 members. These 16 members represent a major cross section of the Aerospace and Electronic Industries. This activity will continue to grow and is all being achieved with external support including additional major support from several DoD agencies. In fact, the total support in these experimental studies substantially now exceeds our JSEP support. This research is truly guiding a major portion of

this technology in the USA and is extremely important for stealth technology advances. However, these advances were only possible because of the initial JSEP support. This continues to be a case where a small investment of basic research funds have been leveraged to generate much larger support and have achieved major contributions for DoD.

Our target identification work also partially funded at one time under JSEP Time Domain Studies is also being funded by several other agencies including ONR and continues to be rather vigorous. Again, JSEP funds have been leveraged to initiate larger programs which have been supported continuously since JSEP funding was terminated.

Our JSEP research continues to focus on Electromagnetic related topics. There are three major electromagnetics areas that were pursued in the past year and a closely related study in Adaptive Arrays.

The goal of our Diffraction Studies is to not only treat new diffracting mechanisms but also to reduce their complexity so that they can be more readily applied to DoD problems. These mechanisms become exceedingly important as stealth technology advances, i.e., as scattered fields are reduced ever lower. It is the intent to reduce these analyses to the Diffraction Coefficient format so that the solution of scattered/radiated fields for aerospace vehicles will involve the use of these coefficients and differential geometry. Such solutions will then be packaged in a variety of computer codes on other projects as part of a technology transfer mechanism.

This activity has included the generation and use of simplified boundary conditions which are designated as Generalized Impedance Boundary Conditions (GIBC) and Generalized Resistive Boundary Conditions (GRBC). This later case is proving valuable in the design of tapered resistive cards for reducing scattered fields from edges. We are also examining the effect

of terminations for open-ended waveguides and our search for an adequate corner diffraction coefficient continues.

In the past, our Integral Equation Studies have focussed attention on the analysis of penetrable materials used in conjunction with conducting surfaces. These have included various tactics to reduce the computation time required, such as making use of special Green's functions so that only the unknowns are currents in the materials. Our current research in this area involves much more general media and we have been successful in treating chiral and non-linear media via the integral equations approach. These studies, however, are still in their initial stages.

The Hybrid Approach represents novel analyses involving more than one basic technique such as was done originally at the ESL by combining diffraction and integral equations which was one of the earlier such solutions. One of our initial efforts involved the scattering from structures that resembled jet intakes and exhausts. Several decades ago, these were supposedly geometries whose scattering properties would never be treated analytically with any degree of success. Our recent work has been overcoming most of these difficulties as will be seen in the deep cavities discussed in the appropriate section. Both government and industry are becoming the primary supporters for this effort and again JSEP support has been used in the initial stages of study that have been carried to the extent that others are now providing the major funding. Research on more shallow antenna cavities has continued under JSEP support and we expect that this effort will also be of general interest to many.

Another topic of interest here is the electromagnetic properties of stripline systems. To treat such devices rigorously requires the inclusion of a very complex Sommerfeld integral. Asymptotic forms of this integral have been

obtained that greatly simplify such analyses.

These asymptotic forms coupled to a judicious choice of basis functions for appropriate choice of boundary conditions for the geometry (coupler, bend, transformer, etc.) not only simplify the analysis, but contribute substantially to understanding the physical mechanism involved. The Hybrid approach is being used to generate solutions for structures where neither moment method or asymptotics can be expected to produce accurate answers.

The adaptive array studies for the past year have been focussed on four areas including nulling bandwidth of adaptive arrays, packet radio networks using adaptive arrays, array pattern synthesis using adaptive array concepts and element reuse in adaptive arrays. The study of nulling bandwidths has been completed. Through put in packet radio can be improved beyond that obtained previously by use of simultaneous multiple beams. The study of array design using adaptive array concepts has been introduced this year and has proven to be useful in the design of arrays that could not be obtained using classical array techniques. The reuse of antenna elements in an adaptive array involves using the same elements to form a main beam and an auxiliary beam simultaneously. The auxiliary beam would then be used as a side lobe canceller.

Technology transition continues to take several forms for our JSEP program. First, of course, are the students graduating in this program who carry the knowledge gleaned in their research programs to other users. Second, there are the published papers, both oral and written, which generally attract the attention of other DoD sponsoring agencies. Such agencies in turn provide additional funding and in general make use of our JSEP research and extend it to better their own programs.

Yet another method takes the form of computer codes developed under non-JSEP sources that make extensive use of JSEP research. As we have noted previously, the results of all of these studies are of great importance in the analysis and control of the scattering from complex shapes.

This continues to be a major task at The Chio State University ElectroScience Laboratory (OSU-ESL) which is funded by a variety of DoD agencies. A major objective of the ESL funded by other sources is to provide a general computer code (or codes) for the evaluation of the RCS of Aerospace vehicles, but a variety of theoretical analysis must be generated before this goal can become a reality. The OSU-ESL continues to provide to DoD users a variety of complex computer codes at the cost of materials for radiation from antennas on aircraft, reflector antennas and integral equation formulations based on previous research activities to 65 industrial organizations with DoD approval for use in DoD activities. In fact, last year 117 additional copies of these very complex user friendly codes were issued. Revised versions incorporating newer results are in progress at this time again as funded by other agencies. Three OSU personnel involved in JSEP are members of an advisory committee to assist in plans for a DoD consortium to develop major vehicular scattering codes. JSEP personnel and concepts developed and those currently being pursued with our JSEP support are expected to play a substantive role in these plans.

III. DIFFRACTION STUDIES

Researchers:

R.G. Kouyoumjian, Professor	(Phone: 614/292-7302)
P.H. Pathak, Associate Professor	(Phone: 614/292-6097)
R. Rojas, Senior Research Assoc.	(Phone: 614/292-2530)
R. Tiberio, Visiting Professor, U. of Florence, Italy	
K.C. Hill, Graduate Research Assoc.	(Phone: 614/294-9283)
H.C. Ly, Graduate Research Assoc.	(Phone: 614/294-9281)
G. Zogbi, Graduate Research Assoc.	(Phone: 614/294-9283)

1. Introduction

The research in diffraction studies is primarily aimed at developing uniform geometrical theory of diffraction (UTD) analysis of new and important canonical problems which serve to significantly extend the capabilities of ray methods for treating EM radiation and scattering from electrically large complex objects.

During the past period, substantial progress has been made in the development of uniform asymptotic high frequency (or UTD) analysis of the diffraction by both perfectly conducting and non-conducting canonical shapes, as well as in the development of beam and ray solutions for propagation within arbitrarily shaped waveguide cavities; all of these topics are of importance to present and future EM technology. These accomplishments are described below.

2. Research Progress

a. Diffraction by Non-Conducting and Penetrable Surfaces

A study of the high frequency diffraction by non-conducting and penetrable surfaces can be performed systematically be developing a set of simpler equivalent boundary conditions for characterizing such surfaces. The development of these boundary conditions then allows the use of certain special techniques (such as the Wiener-Hopf method, or the Generalized Reflection Method) for analyzing the phenomenon of electromagnetic (EM) scattering from discontinuities in these surfaces. It is necessary to develop these higher order boundary conditions for non-conducting opaque surfaces, referred to here as the generalized impedance boundary conditions (GIBC) and the related generalized resistive boundary conditions (GRBC) for penetrable surfaces, because the thin material (dielectric/ferrite) boundaries cannot, in general, be replaced by simple Leontovich impedance or resistive boundary conditions.

A number of useful canonical scattering configurations have been analyzed recently using the GIBC/GRBC, and solutions in the format of the uniform geometrical theory of diffraction (UTD) have been obtained for these cases; in particular, these cases involve the diffraction by:

(a) magnetic dielectric half-plane;

(b) partially coated perfectly conducting half-plane;

(c) two- and three-part planar material boundaries; and

(d) material half-plane with slowly varying electrical properties.

An analysis of the configurations in (b) and (c) above provide the building blocks required to synthesize a high frequency solution for analyzing the

scattering by a thin material slab (by itself or backed by a perfect electric conductor) with slowly varying electrical properties as in (d) above if one replaces the latter configuration by sections of piecewise constant electrical properties; this has also been achieved recently.

Another type of coating that can be used besides magnetic dielectrics is chiral material which has interesting electromagnetic properties. This type of material has been known to exist at optical frequencies; however, it appears now that materials can be built which exhibit chiral properties at microwave frequencies. As it was done for magnetic or dielectric coatings, equivalent boundary conditions suitable for diffraction problems for chiral materials are being developed. It is also helpful to develop integral equations for the scattering by chiral objects to better understand its electrical properties. Integral equations with fewer unknowns than the one developed by Newman et. al. have been developed for three as well as two dimensional bodies.

b. Scattering by Open-Ended Waveguide Cavities

The subject of high frequency EM scattering from a termination inside an open-ended waveguide cavity illuminated from the exterior is a complex one. It is noted that for electrically large waveguide cavities one requires a large number of modes to describe the fields coupled into the cavity from the plane wave incident at the open end. Furthermore, for waveguide cavities of arbitrary shape, the modes cannot even be defined in the conventional sense. Also, a conventional geometrical optics (GO) ray tracking method when applied to calculate the fields coupled from the externally incident plane wave at the open end to the interior cavity region requires one to include many ray bounces for each one of a large number of ray

tubes launched into the cavity. In addition, the conventional GO approach neglects the effects of rays coupled into the interior via diffraction of the waves incident at the edges of the open end. Hence, a field expansion for the interior cavity region in terms of a set of well focussed Gaussian beams (GB's) which overcomes the limitations of the modal and GO ray approaches is investigated. The aperture field is first expanded in terms of GB's, and a suitable way to find the coefficients of expansion which correspond to the initial launching parameters of these beams is developed so that they can be tracked approximately like rays along their beam axis to the interior termination via successive reflections at the cavity walls. These GB's which serve as the basis functions and evolve according to beam optics within the cavity need to be tracked only once since this GB expansion is made independent of the incident angle, thereby making the present approach very efficient. However, since these well focussed GB's distort at each bounce off the slowly varying cavity walls, they can be tracked axially (as a single real ray rather than as complex rays) with reasonable accuracy as long as the length of the cavity (from the open end to the termination) is not much more than four times the average width of the cavity at the open end. A generalized ray expansion (instead of the beam expansion) is also being investigated to overcome this difficulty of the beam approach. Extensions of this beam and ray approaches which have been developed for the two-dimensional case are currently being investigated for the more general three dimensional case.

c. Diffraction by a Corner in a Perfectly Conducting Planar Surface

Work is continuing in developing a useful asymptotic high frequency analysis for the diffraction by a corner in a perfectly-conducting planar surface illuminated by an EM plane wave. While this has been a difficult task, some progress was reported previously; this progress is continuing into the present period where an integral representation has been obtained in which the integrand is expressed in terms of functions which need to be tabulated. It is hoped that this recent development will lead to a result which, unlike previous analyses, is uniform across the various shadow boundary transition regions within the physical optics approximation. A correction to the physical optics approximation is also being investigated which may also work close to grazing on the planar surface containing the corner.

d. Equivalent Currents for Re-Entry Type Bodies

An investigation of the scattered fields of re-entry bodies was initiated on another project. However, the funds to complete this were depleted before the work could be completed. It was deemed to be of sufficient importance to complete using the Director's fund. The study required the extension of the equivalent current concept to include special cone and cone sphere ray paths including combinations of edge, creeping wave and tip diffractions. Previous equivalent currents were restricted to a single mechanism.

3. List of Papers - JSEP Diffraction Studies

Published:

1. P.H. Pathak and R.J. Burkholder, "Modal, Ray and Beam Techniques for Analyzing the EM Scattering by Open-Ended Waveguide Cavities," *IEEE Transactions on Antennas and Propagation*, Vol. 37, No. 5, pp. 635-647, May 1989.

2. R.G. Rojas and P.H. Pathak, "Diffraction of EM Waves by a Dielectric/Ferrite Half-Plane and Related Configurations," *IEEE Transactions on Antennas and Propagation*, Vol. 37, No. 6, pp. 751-761, June 1989.

3. R. Tiberio, G. Pelosi, G. Manara and P.H. Pathak, "High-Frequency Scattering from a Wedge with Impedance Faces Illuminated by a Line Source, Part I: Diffraction," *IEEE Transactions on Antennas and Propagation*, Vol. 37, No. 2, February 1989.

4. R. Tiberio, G. Manara, G. Pelosi and R.G. Kouyoumjian, "High-Frequency Electromagnetic Scattering of Plane Waves from Double-Wedges," *IEEE Transactions on Antennas and Propagation*, Vol. 37, No. 9, pp. 1172-1180, September 1989.

5. R.G. Rojas and Z. Al-hekail, "Generalized Impedance/Resistive Boundary Conditions for Electromagnetic Scattering Problems," *J. Radio Science*, Vol. 24, pp. 1-12, January–February 1989.

6. L. Ersoy and P.H. Pathak, "An Asymptotic High Frequency Analysis of the Radiation by a Source on a Perfectly Conducting Convex Cylinder with an Impedance Surface Patch," *IEEE Transaction on Antennas and Propagation*, Vol. 36, No. 10, pp. 1407-1417, October 1988.

7. C.W. Chuang and M.C. Liang, "A Uniform Asymptotic Analysis of the Diffraction by an Edge in a Curved Screen," *J. Radio Science*, Vol. 23, pp. 781-790, September–October 1988.

8. A.K. Dominek and L. Peters, Jr. "RCS Measurements of Small Circular Holes," *IEEE Transactions on Antennas and Propagation*, Vol. 36, No. 10, October 1988.

Accepted for Publication:

1. P.H. Pathak and M.C. Liang, "On a Uniform Asymptotic Solution Valid Across Smooth Caustics of Rays Reflected by Smoothly Indented Boundaries," *IEEE Transactions on Antennas and Propagation.*

2. O.M. Buyukdura, S.D. Goad and R.G. Kouyoumjian, "A Spherical Wave Representation of the Dyadic Green's Function for a Wedge," *IEEE Transactions on Antennas and Propagation.*

3. H.T. Kim and N. Wang, "UTD Solution for the Electromagnetic Scattering by a Circular Cylinder with Thin Lossy Coatings," *IEEE Transactions on Antennas and Propagation.*

4. J. Choi, N. Wang, L. Peters, Jr. and P. Levy, "Near Axial Back Scattering from a Finite Cone," *J. Radio Science*

Submitted for Publication:

1. R.G. Rojas and L.M. Chou, "Diffraction by a Partially Coated PEC Half-Plane," *J. Radio Science.*

2. H. Ly, R. Rojas and P.H. Pathak, "High-Frequency EM Plane Wave Diffraction by a Planar Two-Part Thin Dielectric/Ferrite Slab," *IEEE Transactions on Antennas and Propagation.*

3. J. Choi, N. Wang, L. Peters, Jr. and P. Levy, "Near Axial Backscattering from a Cone Sphere," *J. Radio Science.*

Papers in Preparation:

1. R.J. Burkholder and P.H. Pathak, "An Analysis of the EM Scattering from an Open-Ended Waveguide Cavity Using Gaussian Beam Shooting."

2. M.C. Liang, P.H. Pathak and C.W. Chuang, "A Generalized Uniform Ray Solution for the Diffraction by a Perfectly-Conducting Wedge with Convex Faces."

3. P.H. Pathak and R.J. Burkholder, "An Analysis of the EM Scattering from Open-Ended Waveguide Cavities Using a Generalized Ray Expansion."

4. R. Rojas, "Integral Equations for the Scattering by an Inhomogeneous Chiral Object."

5. R.G. Rojas, H.C. Ly, P.H. Pathak and R. Tiberio, "EM Plane Wave Diffraction by a Three-Part Thin, Planar Dielectric/Ferrite Slab."

6. H.C. Ly, H. Shamansky and R.G. Kouyoumjian, "Closed Form Solutions for the Elements of the Voltage Matrix in the Moment Method Solution of Linear Antennas."

Conferences/Oral presentations:

1. P.H. Pathak and R.J. Burkholder, "Modal, Ray and Beam Techniques for Analyzing the EM Scattering by Open-Ended Waveguide Cavities," 1989 URSI International Symposium on EM Theory in Stockholm, Sweden, August 14-17, 1989.

2. P.H. Pathak, R.J. Burkholder, R.C. Chou and G. Crabtree, "A Generalized Ray Expansion Method for Analyzing the EM Scattering by Open-Ended Waveguide Cavities," 1989 IEEE AP-Intl. Symposium and URSI Radio Science Meeting, San Jose, California, June 26-30, 1989.

3. R.J. Burkholder and P.H. Pathak, "On the Use of a Beam Method for Analyzing the EM Scattering by Open-Ended Waveguide Cavities," 1989 IEEE AP-Intl. Symposium and URSI Radio Science Meeting, San Jose, California, June 26-30, 1989.

4. R.C. Chou, P.H. Pathak, R.J. Burkholder and G. Crabtree, "On Ray Methods in Computing the EM Scattering from Open-Ended Cavities," 1989 IEEE AP-Intl. Symposium and URSI Radio Science Meeting, San Jose, California, June 26-30, 1989.

5. R.G. Rojas and L.M. Chou, "Diffraction by a Partially Coated PEC Half-Plane," 1989 IEEE AP-Intl. Symposium and URSI Radio Science Meeting, San Jose, California, June 26-30, 1989.

6. R.G. Rojas, "Diffraction by a Partially Coated PEC Half-Plane, " 1989 IEEE AP-Intl. Symposium and URSI Radio Science Meeting, San Jose, California, June 26-30, 1989.

7. G. Pelosi, S. Maci, R. Tiberio, A. Michaeli and R.G. Kouyoumjian, "Improved Equivalent Currents for a Planar Curved Edge," 1989 IEEE AP-Intl. Symposium and URSI Radio Science Meeting, San Jose, California, June 26-30, 1989.

8. J. Choi, N. Wang, L. Peters, Jr. and P. Levy, "Near Axial Backscattering from a Cone Sphere," 1989 IEEE AP-Intl. Symposium and URSI Radio Science Meeting, San Jose, California, June 26-30, 1989.

9. J. Choi, N. Wang, L. Peters, Jr. and P. Levy, "The Backscattered Fields of Finite Conducting Cones," 1989 URSI EM Theory Symposium, Stockholm, Sweden.

Theses & Dissertations

1. H.C. Ly, "A UTD Analysis of the Diffraction by Planar Two and Three Part Configurations Consisting of Thin Dielectric/Ferrite Materials," M.Sc. Thesis, March 1989.

2. R.J. Burkholder, "High Frequency Asymptotic Methods for Analyzing the EM Scattering by Open-Ended Waveguide Cavities," Ph.D. Dissertation, June 1989.

IV. INTEGRAL EQUATION STUDIES

Researchers:

J.H. Richmond, Professor (Phone: 614/292-7601)
E.H. Newman, Associate Professor (Phone: 614/292-4999)
J. Blanchard, Grad. Research Assoc. (Phone: 614/294-9279)
M. Kluskens, Grad, Research Assoc. (Phone: 614/294-9286)

1. Introduction

This section will review the past year's work in integral equation studies. This work has concentrated on developing integral equation and moment method (MM) solutions to electromagnetic radiation and scattering problems involving exotic media. In particular we are analyzing problems involving chiral media and artificial dielectrics.

In this contract period we completed an investigation of the variational technique and its relation to the moment method. The results of this study are summarized in a later section.

A review of the published literature indicates that much of the current research on nonlinear electromagnetics is proceeding in other countries, and the level of this activity is small in comparison with research in nonlinear optics. Therefore we initiated an investigation of microwave interaction with nonlinear media. This work is outlined in a later section, along with some numerical results.

2. Chiral Media

Regardless of the media, electromagnetics is governed by Maxwell's equations:

$$\begin{aligned} \nabla \times \mathbf{E} &= -\frac{\partial \mathbf{B}}{\partial t} \\ \nabla \times \mathbf{H} &= \mathbf{J} + \frac{\partial \mathbf{D}}{\partial t}. \end{aligned} \tag{1}$$

The properties of the media enter through the constitutive relations. For a regular or achiral media,

$$\begin{aligned} \mathbf{D} &= \epsilon \mathbf{E} \\ \mathbf{H} &= \frac{\mathbf{B}}{\mu}. \end{aligned} \tag{2}$$

Here (μ, ϵ) are the permeability and permittivity of the media. If (μ, ϵ) are simple constants, then the media is linear, homogeneous, and isotropic. For a chiral media, the constitutive relations of Equations (2) are generalized to (time harmonic excitation assumed)

$$\begin{aligned} \mathbf{D} &= \epsilon \mathbf{E} + j\zeta \mathbf{B} \\ \mathbf{H} &= \frac{\mathbf{B}}{\mu} + j\zeta \mathbf{E}, \end{aligned} \tag{3}$$

where ζ is referred to as the chiral parameter. The constitutive relations of Equations 3 produce an additional coupling between the electric and magnetic fields, not present in a regular or achiral media. This additional coupling causes a linearly polarized wave to rotate its polarization as it propagates through achiral media.

We have developed an integral equation and method of moments solution to the problem of TM or TE scattering from a chiral cylinder of arbitrary cross section shape. An important first step in this solution was the development of a volume equivalence theorem for chiral media. The chiral volume equivalence theorem allows the chiral scatterer to be replaced by free space and by equivalent electric and magnetic volume polarization currents, $(\mathbf{J}, \mathbf{M})$. By enforcing the volume equivalence theorem, one obtains two coupled vector integral equations for $\mathbf{J}$ and $\mathbf{M}$. These coupled integral equations are then solved for $\mathbf{J}$ and $\mathbf{M}$ using the MM. Once these currents are known, such quantities as the scattered fields or the fields in the chiral cylinder can be found in a fairly straight forward manner.

A second problem involving chiral media is the development of a recursive eigenfunction solution for scattering by a multilayer circular chiral cylinder (with or without a center perfectly conducting core) for TM or TE plane wave incidence. The solution is particularly simple in that it requires the manipulation of order 4 matrices, regardless of the number of layers in the multilayer cylinder. This exact eigenfunction solution has been used to verify the accuracy of the MM solution described above.

Figure 1 shows the MM (dashed line) and eigenfunction (solid line) solution for the TE bistatic echo width of a circular chiral cylinder. If this had been an achiral cylinder, then the scattered magnetic field would have been pure H_z, i.e., the same polarization as the incident wave. However, in Figure 1 note that the chirality of the cylinder rotates the polarization of the field, producing a significant H_ϕ scattered magnetic field. For purposes of comparison, Figure 1 also shows the echo width of the achiral cylinder obtained by setting $\zeta = 0$.

3. Artificial Dielectrics

An artificial media is created by placing a large number of small scatterers per cubic wavelength in some homogeneous host or ambient media. These scatterers may be small dipoles, loops, spheres, etc. An artificial chiral media can be produced by using small helices. When an electromagnetic wave hits the scatterers, it induces currents which behave as small electric or magnetic dipoles. These electric or magnetic dipoles alter (usually increase) the permittivity and permeability of the host media. Often one can design an artificial media with a given permittivity and/or permeability more easily than designing a standard dielectric/ferrite media.

Our research is concerned with determining the permittivity of an artificial dielectric. To do this, we consider the propagation of an electromag-

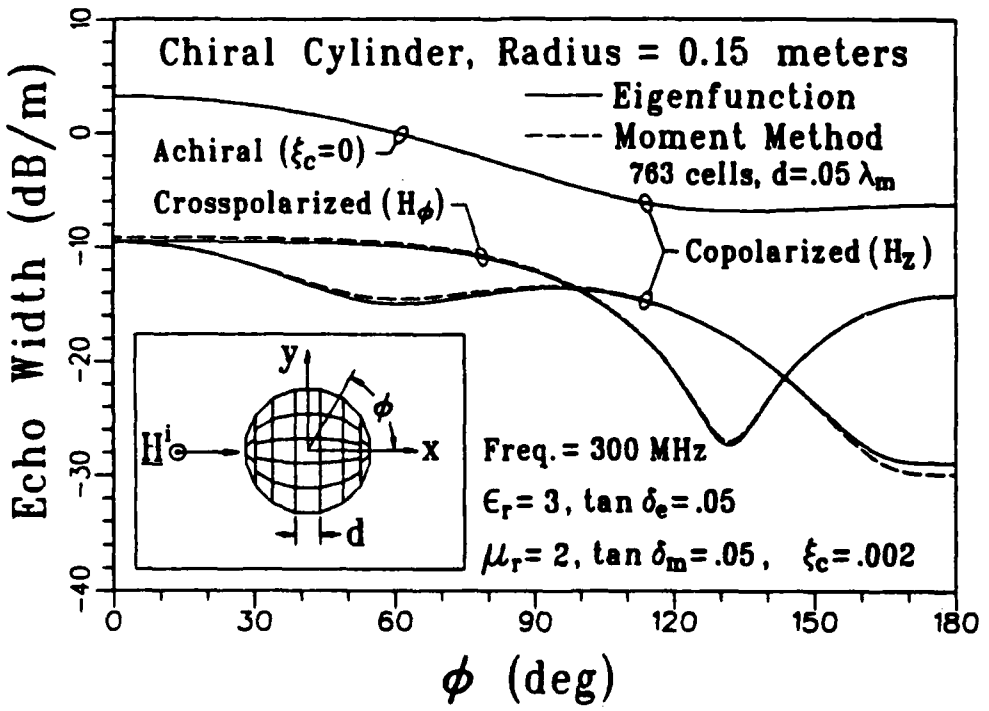

Figure 1: The copolarized and crosspolarized bistatic echo width of a circular chiral cylinder for TE to z incident plane wave.

netic wave through a triply infinite periodic array of scatterers. Using the periodic moment method, one can formulate an integral equation and MM solution to this problem in terms of the current on a single element in the array. By setting the determinant of the MM impedance matrix to zero, one can determine the normal modes of the array, which in turn can be used to determine the equivalent dielectric constant of the artificial media. We have successfully applied this method to the 2D problem of a periodic array of thin dielectric rods. At present we are applying the method to the 3D problem in which the scatterers are simple dipoles.

4. Variational Properties of the Moment Method

It has long been known that the variational method offers significant advantages in the solution of problems concerning electrostatics and TEM transmission lines. It has generally been assumed that these advantages extended also to problems concerning antennas and scattering, and therefore the variational method came into widespread use in these areas during the 1950's.

In the 1960's the moment method was introduced in the electromagnetics area, and soon it replaced the variational method as the "method of choice." Recently we discovered that the moment method does not always exhibit the variational property, so we undertook an investigation to answer the following questions:

a. Under what conditions does the moment method possess the variational property?

b. When the moment method is variational, precisely which quantities are stationary?

c. Do the variational moment methods offer any significant advantage over the nonvariational moment methods?

As a result of our investigation, we wrote a paper on the subject and submitted it for publication. Let us summarize the results presented in this paper. We found that the following quantities can be expressed in terms of the self reaction or the mutual reaction of the currents induced on the surface of the antenna or scatterer: impedance, admittance, gain and radar cross section. Thus, the stationarity of these important quantities hinges on the stationarity of the reaction. The reaction is stationary with Galerkin's method, but not when calculated with the non-Galerkin moment methods in the customary manner. However, stationarity can be regained by employing the basis and testing functions in a symmetric fashion.

In most examples, the variational moment methods do offer a significant advantage in accuracy and rate of convergence. For antennas and scattering, however, this advantage is not as great as in electrostatic and TEM problems.

Let **J** denote the exact current distribution induced on a conducting surface. Then we may represent the approximate current distribution $\mathbf{J_a}$ as follows

$$\mathbf{J_a} = C[\mathbf{J} + p\mathbf{e}] \tag{4}$$

where p is an adjustable parameter and **e** is essentially the "error" or the difference between the correct and approximate current distributions. The constant C is determined via the moment method. As a function of the parameter p, Figure 2 illustrates the self reaction as calculated with Galerkin's method and a non-variational moment method. When p is zero, both methods yield the correct solution for the reaction. As p departs from zero, it

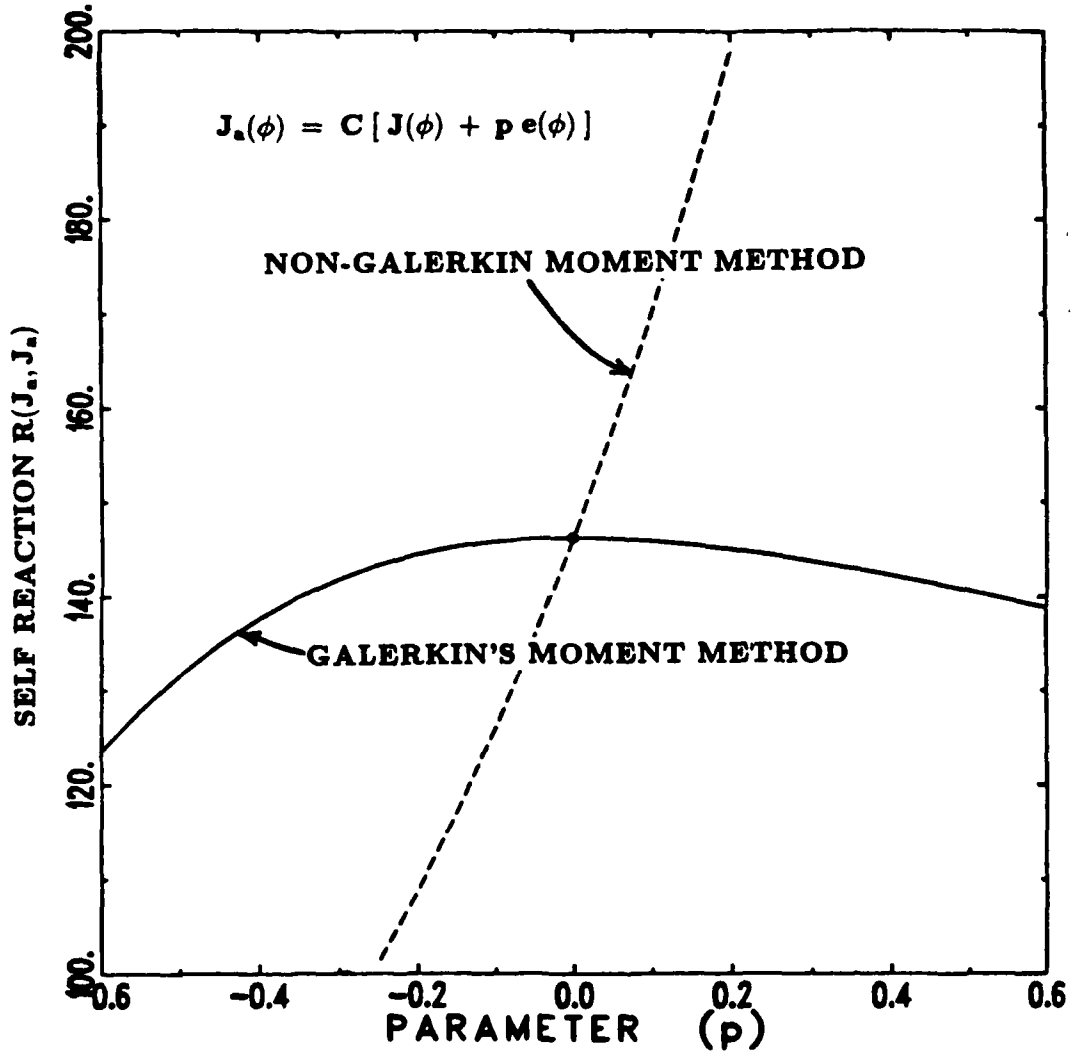

Figure 2: Self reaction versus the parameter p.

may be observed in Figure 2 that the solution error increases slowly with Galerkin's method and rapidly with the non-variational moment method. By definition, a solution is variational (or "stationary") if the rate of change vanishes as p tends toward zero.

In the moment method, one solves a system of N simultaneous linear equation with N unknowns. As a function of N, Figure 3 illustrates the calculated susceptance per unit length for an axial slot antenna on a circular cylinder. In this example, Figure 3 shows that the variational moment method provides greater accuracy and faster convergence than the non-variational moment method.

5. Nonlinear Media

We are interested in the interaction of electromagnetic microwaves with nonlinear devices and nonlinear media. Such interactions have potentially useful applications, but very little effort is currently devoted to this area. In the past 36 years, the nonlinear area has been represented in IEEE Transactions on Antennas and Propagation only by a few papers on the following subjects:

a. Scattering by a single dipole with nonlinear load,

b. EMP transmission through a ferromagnetic shield, and

c. Nonlinear plasmas.

On the other hand, the areas of nonlinear optics and nonlinear circuits show considerable activity.

A section on nonlinear media was included in The 1989 URSI International Symposium on Electromagnetic Theory. This section consists of four

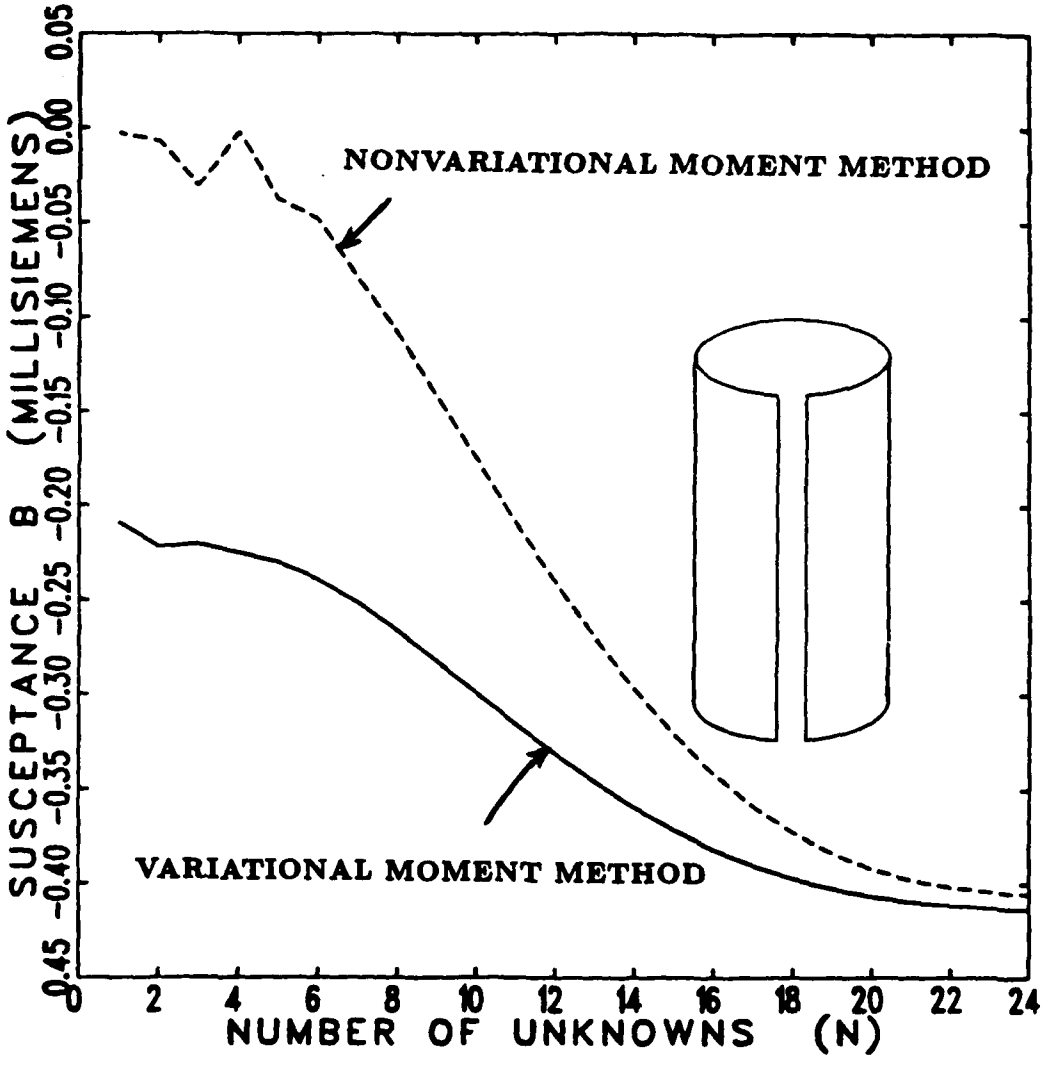

Figure 3: Susceptance of axial slot versus matrix size.

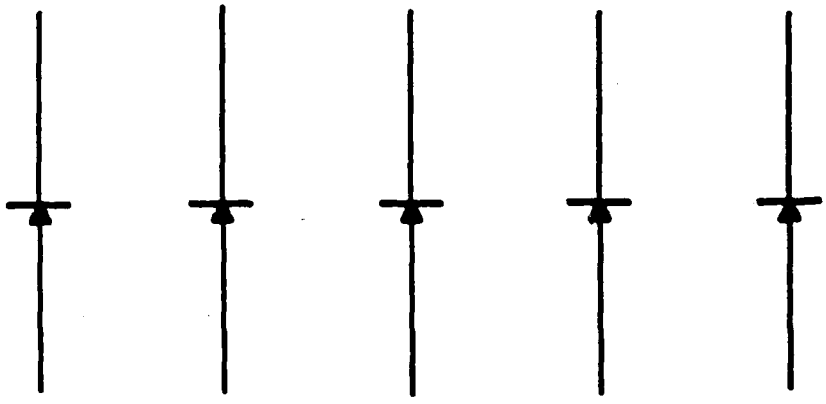

Figure 4: Periodic planar array of dipoles with nonlinear loads.

papers from Russia and one paper each from Greece, Italy, Poland, Scotland and Sweden. Out of these nine papers, three are concerned specifically with nonlinear optics.

In this contract period we investigated plane-wave scattering by a periodic planar array of parallel wire dipoles. As illustrated in Figure 4 the

single row of dipoles forms a broadside array, and each dipole has a nonlinear load. The load may be series-opposing diodes to represent a nonlinear capacitor, or parallel-opposing diodes to represent a nonlinear resistor. Several time-harmonic plane waves may simultaneously be incident on the array, but each wave has the same direction of propagation and the frequencies are harmonically related. In the steady-state condition the total field is thus periodic in space and time, and Floquet's theorem is applicable.

Even though the incident wave contains only a few harmonic frequencies, the scattered field will contain an infinite series of harmonics. This series may be truncated, however, and we wish to solve numerically for the complex amplitudes of the various harmonic plane waves scattered (or reflected) in the specular direction. One may also be interested in the amplitudes of some of the grating lobes.

The solution of this problem is simplified by splitting it into two parts. In Part I the nonlinear loads are removed, and we apply the moment method to solve the scattering problem where a time-harmonic plane wave has oblique incidence on a periodic planar array of dipoles with short-circuited terminals. This procedure is carried out for each harmonic wave incident on the array. For the nth harmonic, one calculates and stores the open-circuit received voltage V_n^r induced in the dipoles.

Part I also includes the solution of a phased-array transmitting problem. Again the nonlinear loads are removed, and a one-volt generator is placed at the terminals of each dipole. The moment method is then applied to solve this time-harmonic transmitting problem. This procedure is carried out for each harmonic frequency deemed to be significant in the representation of the total scattered field. For the nth harmonic, one calculates and stores the active antenna impedance Z_n.

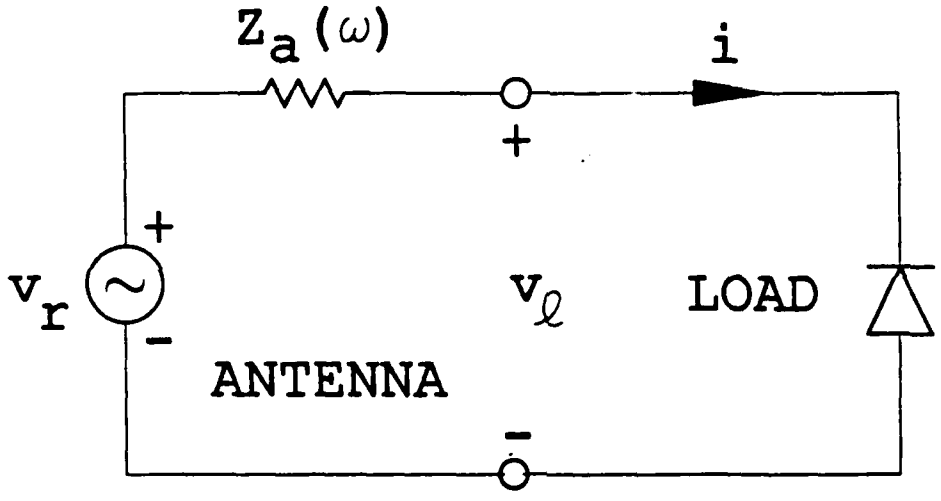

Figure 5: *Thevenin equivalent circuit for dipole array with nonlinear loads.*

Figure 5 illustrates the Thevenin equivalent circuit for a dipole array with nonlinear loads. The open-circuit received voltage $v_r(t)$ and the load voltage $v_\ell(t)$ are expanded in Fourier series as follows:

$$v_r(t) = Real \sum_n V_n^r \exp(jn\omega_o t) \tag{5}$$

$$v_\ell(t) \;=\; Real \sum_n V_n^\ell \exp(jn\omega_o t) \tag{6}$$

Of course, the active antenna impedance $Z_a(\omega)$ is frequency dependent, and Z_n denotes its value at the nth harmonic frequency. From the basic circuit laws, the load current is given by

$$i(t) \;=\; Real \sum_n [(V_n^r - V_n^\ell)/Z_n] \exp(jn\omega_o t) \;=\; i_1(t) \tag{7}$$

Now the load current $i(t)$ and the load voltage $v_\ell(t)$ must be related by the characteristics of the nonlinear load. If each dipole is loaded with matched parallel-opposing diodes, the current-versus-voltage law may be represented as follows:

$$i(t) \;=\; \sum_{n=1,3,5} c_n [v_\ell(t)]^n \;= i_2(t) \tag{8}$$

The analysis may be extended to take account of the load inductance and capacitance, but this detail will not be covered here.

At the outset, one is given the angle of incidence, the frequency, and the complex amplitude of each incident plane wave. The impedances Z_n and the received voltages V_n^r are then calculated as Part I of the analysis. The object of Part II is to determine numerically the load voltages V_n^ℓ. This is accomplished as follows.

From Equations (7) and (8), the currents $i_1(t)$ and $i_2(t)$ must be equal to each other and to $i(t)$. In a least-square solution, one adjusts the voltages V_n^ℓ to minimize the quantity F which is defined as follows:

$$F \;=\; \int_0^T [i_1(t) - i_2(t)]^2 \, dt \tag{9}$$

where $T \;=\; 2\pi/\omega_o$ denotes the basic period of the waveform. We have found the gradient search technique to be accurate and efficient for minimizing F. After the load voltages V_n^ℓ and load currents I_n have been determined in this manner, it is a simple matter to calculate the amplitude of the reflected wave and the grating lobes scattered by the periodic structure.

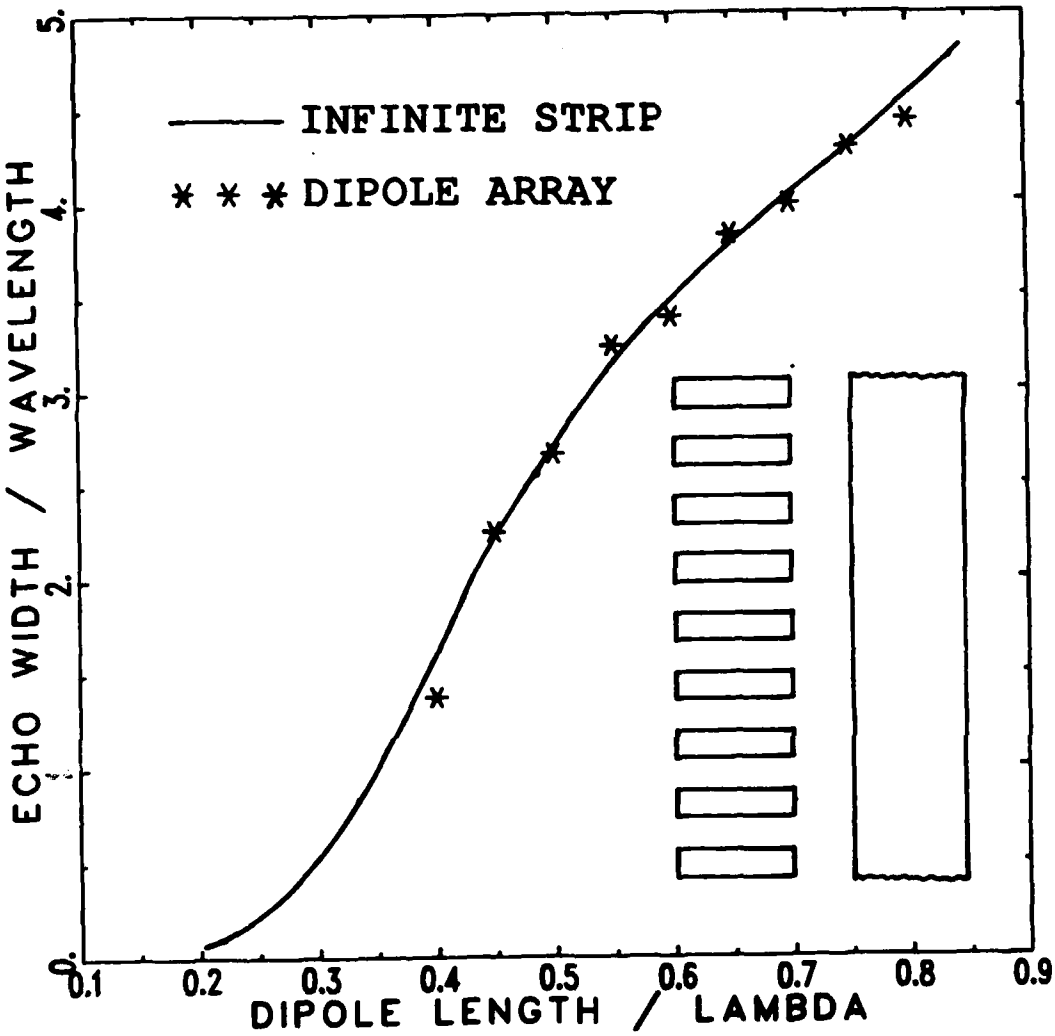

Figure 6: Broadside backscatter versus length for dipole array and infinite strip.

Figure 6 illustrates the backscatter echo width for a periodic array of short-circuited dipoles with broadside incidence, as calculated with our new computer program which was developed as part of this study. For comparison Figure 6 also shows the exact backscatter echo width for a perfectly

conducting strip with infinite length, and the close agreement between the two results tends to verify the accuracy of the calculated data. In Figure 6 the dipoles are thin planar strip dipoles, the dipole width is 0.04 wavelengths, and the aperture width is also 0.04 wavelengths. Of course, when the aperture width is increased, the backscatter characteristics of the dipole array no longer resemble those of the infinite conducting strip.

Figure 7 illustrates the load currents $i_1(t)$ and $i_2(t)$ defined in Equations (7) and (8). The close agreement between the two calculated current waveforms tends to verify the accuracy of the solution, which was obtained with the gradient search technique. This example was designed as a preliminary test of the gradient search program, with the active antenna impedance taken to be a pure resistance of 100 ohms. To simulate a dipole array with two frequencies incident, the open-circuit voltages were taken to be 2 volts at frequency $2\omega_o$ and 0.2 volts at $3\omega_o$. The nonlinear load characteristic was taken to be:

$$i(t) = (v_\ell + 0.5v_\ell^3)/1000 \tag{10}$$

This investigation of the single-row periodic dipole array will be completed in the next contract period. Our program for the active Thevenin impedance will be refined for improved efficiency and accuracy, and the gradient-search program will be extended to optimize the phase as well as the amplitude of each harmonic load voltage V_n^ℓ. Far-zone scattering data will be compiled to illustrate some of the interesting results obtainable with this configuration, and a paper will be submitted for publication. In addition we will undertake an investigation of scattering by a doubly periodic planar array of dipoles with nonlinear loads, as illustrated in Figure 8.

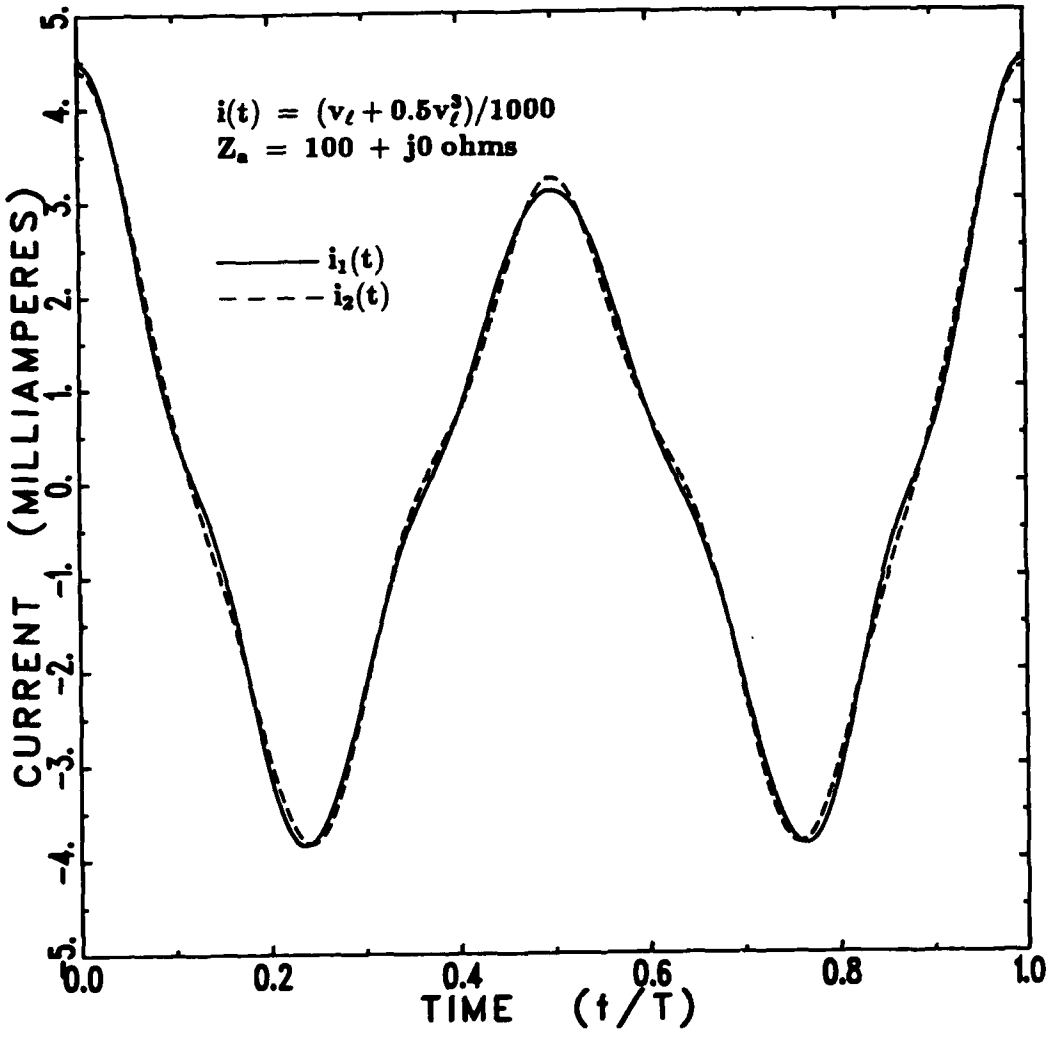

Figure 7: Current through nonlinear load with two frequencies incident.

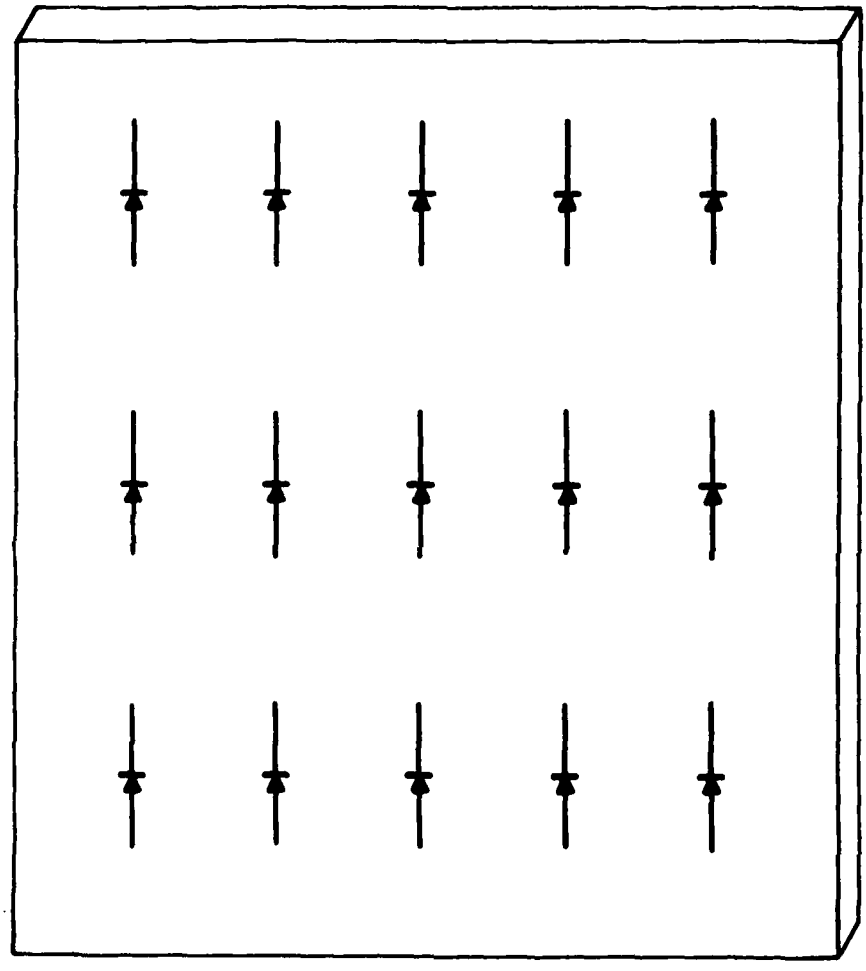

Figure 8: Doubly periodic array embedded in dielectric slab.

6. Other Research

In addition to the above research, we have:

1. prepared an invited paper for *Electromagnetics* describing our surface patch modeling techniques . These techniques were developed in part under past JSEP support.

2. worked on the preparation of a reprint book on the method of moments (E.H. Newman, E.K. Miller and L. Mitschang). A proposal for the publication of this book has been submitted to IEEE Press.

7. List of Papers - JSEP Integral Equation Studies

Published:

1. J.H. Richmond, "Scattering by a Conducting Elliptic Cylinder with Dielectric Coating," *J. Radio Science*, Vol. 23, pp. 1061-1066, November 1988.

2. E.H. Newman, "Generation of Wideband Data from the Method of Moments by Interpolating the Impedance Matrix," *IEEE Transactions on Antennas and Propagation*, Vol. 36, No. 12, pp. 1820-1824, December 1988.

3. J.L. Blanchard and E.H. Newman, "Numerical Evaluation of Parabolic Cylinder Functions," *IEEE Transactions on Antennas and Propagation*, Vol. 37, No. 4, pp. 519-523, April 1989.

4. E.H. Newman and R.J. Marhefka, "Overview of MM and UTD Methods at The Ohio State University," *Proceedings of the IEEE*, Vol. 77, No. 5, May 1989.

Accepted for Publication:

1. J.H. Richmond, "Axial Slot Antenna on Dielectric-Coated Elliptic Cylinder," *IEEE Transactions on Antennas and Propagation*, Vol. 37, October 1989.

2. M.S. Kluskens and E.H. Newman, "Scattering by a Chiral Cylinder of Arbitrary Cross Section," *IEEE Transactions on Antennas and Propagation.*

Submitted for Publication:

1. J.H. Richmond, "On the Variational Aspects of the Moment Method," *J. Radio Science.*

2. E.H. Newman, "Polygonal Plate Modeling," *Electromagnetics*, invited paper.

Papers in Preparation:

1. J.H. Richmond, "Scattering by Periodic Dipole Array with Nonlinear Loads."

2. M.S. Kluskens and E.H. Newman, "Scattering by a Multilayer Chiral Cylinder."

3. J. Blanchard and E.H. Newman, "Method of Moments Analysis of Artificial Media."

Conferences/Oral Presentations:

1. M. Kluskens and E.H. Newman, "Scattering by an Arbitrary Cross Section Chiral Cylinder," presented at the 1989 IEEE AP-Intl. Symposium and URSI Radio Science meeting, San Jose, California, June 26-30, 1989.

V. HYBRID STUDIES

Researchers:

P.H. Pathak, Associate Professor (Phone: 614/292-6097)
R.C. Chou, Assistant Professor (Phone: 614/292-7298)
M. Marin, Fullbright Post-Doc. Feilow from Spain (during 1987-1989)
M. Hsu, Grad. Research Assoc. (Phone: 614/294-9280)
P. Munk, Grad. Research Assoc. (Phone: 614/294-9285)
L.M. Chou, Grad. Research Assoc. (Phone: 614/294-9280)

1. Introduction

A goal of this research is to develop useful and efficient combinations of different hybrid techniques for analyzing a variety of electromagnetic (EM) radiation and scattering phenomena that would otherwise be either impossible or cumbersome to treat via any one technique.

During the past period, substantial progress has been made in the development of hybrid analysis for efficiently treating the EM phenomena associated with planar microstrip configurations and with antenna cavities. In addition, an effort has been initiated to develop a hybrid procedure for dealing with the EM scattering by complex shapes. These accomplishments are described below.

2. Research Progress

a. Hybrid Analysis of Microstrip Configurations

An analysis of microstrip phenomena involving microstrip antennas/arrays, feed networks, circuits, etc. can be handled not only in a more efficient manner via the hybrid combination of moment method and asymptotic high frequency techniques developed under JSEP, but it also provides a better

physical insight into the surface, leaky and space waves effects which remain hidden in the conventional moment method approach employing the exact Sommerfeld integral form of the microstrip Green's function. This work has continued to include planar double layer substrate/superstrate microstrip configurations and an initial study has also begun to extend these hybrid concepts to deal with single layer conformal circularly cylindrical microstrip structures.

At present, hybrid methods are being developed to characterize various types of microstrip components and discontinuities with the aid of the recently developed asymptotic closed form of the planar microstrip Green's function for one or two layer configurations. In order to further enhance the efficiency of the full wave (moment method) analysis of such structures, besides employing the closed form asymptotic microstrip Green's function, is to choose a mixed set of only a few basis functions for accurately representing the current on the microstrip geometries (e.g. couplers, bends, transformers, feed lines, etc.);this requires far fewer basis functions than is done in conventional moment method approaches. It would be of interest to use the conventional sub-sectional (or some other equivalent) basis set only near the microstrip discontinuity; whereas, away from this discontinuity, a proper entire domain basis set involving well chosen known functional forms needs to be used to drastically cut down the number of unknowns in the moment method analysis. These entire domain basis set would clearly have to depend on the nature of the specific microstrip configuration under study.

While a useful conformal circular cylindrical microstrip antenna configuration has been analyzed recently, and a very efficient solution obtained for an electrically large cylinder, it is primarily valid for just a few elements

not separated too far from each other. It is therefore desirable to arrive at an asymptotic closed form microstrip Green's function which is not only valid for electrically large cylinders and for larger arrays, but also valid for arbitrarily curved convex boundaries. Work has now been initiated to deal with this more difficult conformal microstrip array configuration.

b. Hybrid Analysis of EM Scattering by Antenna Cavity Configurations

A hybrid combination of asymptotic high frequency and modal techniques was developed within the framework of the generalized scattering matrix formulation earlier under partial JSEP support to analyze the EM scattering by two-dimensional (2-D) antenna cavity shapes for which the cavity modes can be found analytically. Recently, that approach has been extended to include the effect of dominant mode waveguide fed antennas within the cavity; this is achieved by finding only the scattering matrices which characterize the reflection and transmission of waves across any given waveguide fed aperture (in the cavity back wall) using a moment method procedure. The mutual coupling effects between an array of waveguide fed slots are then found quite easily. The rest of the effects (dealing with the open end of the cavity) are found via asymptotic high frequency methods. It is noted that a conventional moment method analysis of the scattering by the entire waveguide fed array in the cavity environment would be far more cumbersome and physically far less appealing than the present hybrid procedure. The dominant mode waveguides are terminated in loads which must be adjusted so as to control the backscattering in some desired fashion. Work is currently under way to optimize these loads in some manner for the reason cited above, and to extend this analysis to treat the scatter-

ing from 3-D waveguide fed apertures in a cavity. Eventually this approach could in a formal sense be extended to treat relatively general antennas located within the cavity.

c. Hybrid Analysis of EM Scattering from Complex Structures

A hybrid combination of asymptotic high frequency and moment method techniques is being developed to analyze the EM scattering from electrically large complex structures which cannot be handled accurately and efficiently by either method above. The first configuration being studied at present is a finite perfectly-conducting plate of relatively arbitrary shape on an electrically large perfectly-conducting convex cylinder. Such a configuration can, for example, simulate a fin on a fuselage of an aircraft or a missile. The moment method will, in this hybrid procedure, be restricted to only the electrically smaller fin portion thereby making the solution very useful and efficient. Other configurations in increasing orders of complexity will also be considered subsequently. For example, as this hybrid procedure is further developed to handle the corner of a plate, then a larger control surface attached to the curved fuselage of an aerospace vehicle can be included in this analysis. In the latter configuration, the unknowns in the moment method will then be restricted only to the junctions between the plate and the curved surface, and to the remaining corners of the plate. More complex shapes could then be built up in this manner as indicated previously.

3. List of Papers - JSEP Hybrid Studies

Published:

1. C.W. Chuang, "Generalized Admittance for a Slotted Parallel Plate Waveguide," *IEEE Transactions on Antennas and Propagation*, Vol. 36, No. 9, pp. 1227-1230, September 1988.

2. P.H. Pathak and A. Altintas, "An Efficient High Frequency Analysis of Modal Reflection and Transmission Coefficients for a Class of Waveguide Discontinuities," *J. Radio Science*, Vol. 23, No. 6, pp. 1107-1119, November–December 1988.

3. M. Marin, S. Barkeshli and P.H. Pathak, " Efficient Analysis of Planar Microstrip Geometries Using a Closed Form Asymptotic Representation of the Grounded Dielectric Slab Green's Function," *IEEE Transactions on Microwave Theory and Technique*, Vol. 37, pp. 669-679, April 1989.

4. C.W. Chuang and P.H. Pathak, "Ray Analysis of Modal Reflection for Three-Dimensional Open-Ended Waveguides," *IEEE Transactions on Antennas and Propagation*, Vol. 37, No. 3, pp. 339-346, March 1989.

Accepted for Publication:

1. S. Barkeshli, P.H. Pathak and M. Marin, "An Asymptotic Closed-Form Microstrip Surface Green's Function for the Efficient Moment Method Analysis of Mutual Coupling in Microstrip Antennas," *IEEE Transactions on Antennas and Propagation.*

2. M. Marin, S. Barkeshli and P.H. Pathak, "On the Location of Proper and Improper Surface Wave Poles for the Grounded Dielectric Slab," *IEEE Transactions on Antennas and Propagation.*

3. A. Nagamune and P.H. Pathak, "An Efficient Plane Wave Spectral Analysis to Predict the Focal Region Fields of Parabolic Reflector Antennas for Small and Wide Angle Scanning," *IEEE Transactions on Antennas and Propagation.*

4. K.D. Trott, P.H. Pathak and F. Molinet, "A UTD Type Analysis of the Plane Wave Scattering by a Fully Illuminated Perfectly-Conducting Cone," *IEEE Transactions on Antennas and Propagation.*

Submitted for Publication:

1. M. Marin and P.H. Pathak, "An Asymptotic Closed Form Representation for the Grounded Double Layer Surface Green's Function," *IEEE Transactions on Antennas and Propagation.*

2. S. Barkeshli and P.H. Pathak, "Radial Propagation and Steepest Descent Path Integral Representations of the Planar Microstrip Dyadic Green's Function," *J. Radio Science.*

Papers in Preparation:

1. P.H. Pathak and R.J. Burkholder, "A Reciprocity Formulation for Calculating the EM Scattering by an Obstacle within an Open-Ended Waveguide Cavity."

2. P. Munk, P.H. Pathak, M.C. Liang and C.W. Chuang, "A Hybrid Analysis of the EM Scattering by Antenna Cavities."

Conferences/Oral Presentations:

1. M. Marin and P.H. Pathak, "A New Integral Representation of the Microstrip Green's Function for Electrically Large Coated Cylinders," 1989 IEEE AP-Intl. Symposium and URSI Radio Science meeting, San Jose, California, June 26-30, 1989.

2. M. Marin and P.H. Pathak, "An Asymptotic Closed Form Representation for the Substrate-Superstrate Green's Function," 1989 IEEE AP-Intl. Symposium and URSI Radio Science meeting, San Jose, California, June 26-30, 1989.

VI. ADAPTIVE ARRAY STUDIES

Researchers:

R.T. Compton, Jr., Professor (Phone: 614/292-5048)
Frederick Vook, Graduate Research Associate
Carl Olen, Graduate Research Associate
Jim Ward, Graduate Research Associate

1. Introduction

During the past year we have done research under the JSEP contract in four areas related to adaptive arrays:

1. Nulling bandwidth of adaptive arrays
2. Packet radio networks with adaptive arrays
3. Array pattern synthesis using adaptive array concepts
4. Element reuse in adaptive arrays

We discuss our progress in each of these areas below.

2. Nulling Bandwidth of Adaptive Arrays

At the beginning of this past year, we completed our study of the nulling bandwidth of linear adaptive arrays with up to 10 elements. This work was described previously in the JSEP Final Report of November 1988 [1] and will be discussed only briefly here.

The nulling performance of an adaptive array is affected by interference bandwidth [2]. Earlier JSEP studies [3] had shown how bandwidth affects the performance of a two-element array and how the degradation can be overcome by using tapped delay-line processing in the array. These studies

also determined how to choose the number of taps and the tap spacing behind the elements and showed that FFT (fast Fourier transform) and tapped delay-line processing are equivalent [4]. During the previous JSEP contract, we extended this work to linear arrays with up to ten elements. Typical results were included in the JSEP Annual Report of 1988 [1].

During the early part of the present contract year, we concluded this work. The result was a M. Sc. Thesis [5] by Mr. F. Vook and a paper submitted for publication to the IEEE Transactions on Antennas and Propagation [6].

3. Packet Radio Networks with Adaptive Arrays

Our second area of research during the past year involves the use of adaptive arrays in multiple access packet radio networks. This work area has been continued from the previous JSEP contract. Our results show that an adaptive array can provide a dramatic improvement in the performance of a simple ALOHA packet radio system. It does this by reducing the effects of packet collisions at the repeater.

Under the previous JSEP contract, we initially considered using an adaptive array that forms one beam in a packet system. We found that a single beam adaptive array yields a substantial improvement in throughput and a corresponding reduction in delay. The improvement is similar to that obtained with Carrier Sense Multiple Access (CSMA) [7], without the requirement that all radio units be able to hear one another as in CSMA.

However, as a result of this work, it became clear that an even more substantial improvement could be obtained by forming two or more beams simultaneously from the same antenna elements. (This is easily done in a digital adaptive array.) In a slotted packet system, a two-beam adaptive array, for example, would lock one beam onto the first packet that arrives in

each slot and a second beam onto the second packet in that slot. Each beam would have a peak response toward one packet and nulls on other packets. This technique allows the array to receive two packets at the same time in the same time slot. The result is a substantial increase in throughput and reduction in delay.

This technique, which makes it possible to achieve average throughputs greater than 1 packet/slot, allows a network with a multiple beam adaptive array (MBAA) to operate at much higher traffic rates than are feasible in a standard ALOHA system. For example, Figures 9-12 compare the average throughput, delay, and backlog performance of systems with no adaptive array and with 1, 2, and 3-beam adaptive arrays at the central repeater node in a 20 node network. These averages are computed by determining the steady state probability distribution of the system state using a Markov chain analysis. In these curves the probability that a given node transmits a new packet, p_{nt}, is varied. The retransmission probability for backlogged packets, p_{rt}, is fixed at 0.5. For the curves with an adaptive array, there are $N = 6$ nulls/beam, the resolution beamwidth is 10°, and the uncertainty interval in the beginning of each slot is 61 bits long.

Figure 9 shows the delay-throughput curve. Without an adaptive array, the delay increases without bound for very low p_{nt}. The corresponding curve (not shown in the figure) lies nearly along the vertical axis and is not discernible. As an adaptive array is added and the number of beams is increased, higher throughputs and lower delays are achieved. A 2-beam adaptive array can provide an average throughput of 1.4 packet/slot at an average delay of 3.1 slots for $p_{nt} = 0.089$, while the 3-beam MBAA gives a maximum average throughput of 2.15 packets/slot at an average delay of 2.2 slots for $p_{nt} = 0.141$. By comparison, at the same new packet generation

rate, a slotted system with no adaptive array has an average throughput of 0.00002 packets/slot and an average delay of 1×10^6 slots.

Figure 10 shows the average throughput versus p_{nt}. Without an adaptive array, the throughput is nearly zero for all p_{nt}, so the curve for no adaptive array is barely visible. (The retransmission probability is too high for standard slotted ALOHA.) As the number of beams increases the average throughput also increases. If p_{nt} is increased past the point where the throughput is maximum, the throughput does not go to zero but approaches a constant value. This value is the throughput obtained when all nodes are backlogged, and the number of successful packets depends only on the retransmission probability.

Figure 11 shows the average delay versus p_{nt}. Again, the curve for standard slotted ALOHA increases very rapidly and is not visible. As more beams are added, the system can be operated with higher p_{nt} (higher traffic) while maintaining a reasonable delay performance.

Finally, Figure 12 shows the average number of backlogged stations as a function of p_{nt}. Without an adaptive array, the network becomes completely backlogged almost as soon as $p_n t$ is increased above zero. With an MBAA, the backlog decreases as more beams are added because more packets are successful per slot. When the average number of packets per slot becomes greater than the number of beams, the MBAA system is overloaded and will become highly backlogged. For $p_{nt} > 0.15$, performance for the 3-beam case begins to degrade.

In general, the throughput, delay and stability performance of a packet system using an adaptive array improves as more nulls per beam are added, as the uncertainty interval increases, and as the antenna beamwidth decreases. Increasing the length of the uncertainty interval improves perfor-

mance by causing more packets to be acquired. Reducing the beamwidth of the array also increases performance by increasing the number of acquired packets that are eventually successful. The ideal case of an infinite uncertainty interval (or zero bit duration) and zero beamwidth (infinite array resolution) corresponds to perfect capture; in this case a K beam system would have a maximum throughput of K packets/slot.

4. Array Pattern Synthesis Using Adaptive Array Concepts

During the past year, we have developed a new method of designing array patterns to meet a given sidelobe specification. This method is based on adaptive array concepts. This work resulted in one M.Sc. Thesis [8] and a paper submission [9]. We summarize this work below.

The problem of synthesizing antenna patterns with low sidelobes is a long-standing problem. In a classic paper, Taylor [10] obtained an aperture distribution for a continuous aperture that produces equal height sidelobes near the main beam and tapered far out sidelobes. Hyneman and Johnson [11,12] presented techniques for controlling pattern behavior by moving zeros in the pattern function. Additional contributions include the work of Elliott [13,14,15], and White [16].

For arrays, the classic paper of Dolph [17] derived the weights required in a uniformly spaced linear array to obtain minimum beamwidth for a given maximum sidelobe level and showed that the patterns are obtained from Chebyshef polynomials. Other contributions to the pattern synthesis problem for arrays include the work of Villeneuve [18] and Elliot and Stern [19].

An important feature of all these techniques is that they are applicable only to arrays of *uniformly spaced, isotropic* elements. None can address

design problems in which the elements are nonuniformly spaced, the element patterns are unequal, or the elements do not lie along a straight line.

Under the JSEP contract, we have developed a simple numerical synthesis technique that can be used with arrays of *arbitrary* elements. This technique allows one to find a set of weights to steer a beam in a given direction and meet an arbitrary sidelobe specification in other directions.

The underlying approach is to assume that the array elements are used as elements in an adaptive array [2,20]. The main beam is steered in the desired direction by choosing the steering vector for that direction. To reduce the sidelobes, a large number of interfering signals is assumed to be incident on the array from the sidelobe region. The number of interfering signals M is made much larger than the number of degrees of freedom in the array. On a computer, one solves for the resulting adapted weights and the adapted pattern. This pattern is then compared with the design objectives. At any angle where the sidelobes are too high or too low, the interference power is increased or decreased accordingly and then the weights are recalculated. This process is repeated iteratively until a suitable final pattern is obtained. The final adapted weights are then used as the design weights for the actual (nonadaptive) array.

Because this method is a numerical technique, it does not yield analytic solutions for the weights. However, being a numerical technique, it can be used with much more general types of problems than an analytical approach. The method easily handles arrays in which the element patterns of different elements are different and the element locations are arbitrary. It can be used to obtain patterns whose sidelobe levels vary arbitrarily with angle.

The actual procedure is as follows. Suppose the design goal is to have the

sidelobes at angle θ be $D(\theta)$ dB below the beam peak. For the initial step, the powers of all M interference signals are set to zero, so the only undesired output is the thermal noise. The adapted weights and the resulting pattern are calculated. This initial step is the $k = 0$ iteration.

For subsequent iterations, when the array has a pattern $p(\theta, k)$, we define $P(k) = \max_\theta\{p(\theta, k)\}$ to be the magnitude of the *beam peak* at iteration k. We denote the angles of the first nulls (or minima) on each side of the beam peak by $\theta_L(k)$ and $\theta_R(k)$, respectively. The *beam region* is the region $\theta_L(k) \leq \theta \leq \theta_R(k)$, and the *sidelobe region* is the region outside the beam region.

At each succeeding iteration, the sidelobe level of the pattern is compared with the desired sidelobe level $D(\theta)$ and the interfering signal powers are adjusted accordingly. Suppose θ_{i_m} denotes the arrival angle for interference signal m, where $m = 1, 2, \ldots, M$. If the sidelobe level of the pattern at angle θ_{i_m} is above the desired sidelobe level $D(\theta_{i_m})$, the interference power at angle θ_{i_m} is increased. If the sidelobe level at θ_{i_m} is below $D(\theta_{i_m})$, the interference power is decreased. Negative interference powers are not allowed, so if an interference power would become negative it is set to zero.

Before assigning interference powers, it is necessary to find the current desired voltage envelope $d(\theta_{i_m}, k)$ at each iteration. $d(\theta_{i_m}, k)$ is related to $D(\theta_{i_m})$ and the current beam peak $P(k)$ by

$$d(\theta_{i_m}, k) = \frac{P(k)}{10^{[D(\theta_{i_m})/20]}}. \tag{11}$$

$d(\theta_{i_m}, k)$ must be recalculated for each iteration because the beam peak $P(k)$ is a function of k. (Although interference is not added in the beam region, the magnitude of $P(k)$ changes at every iteration.)

It is also necessary to calculate the limits of the current beam region, $\theta_L(k)$ and $\theta_R(k)$, at each iteration. These angles continually change, be-

cause the beam width widens as the sidelobes are reduced. $\theta_L(k)$ and $\theta_R(k)$ are needed so that interference can be kept out of the main beam. The interference arrival angles θ_{i_m} are chosen to be uniformly spaced across all angles, including the main beam region. But then at each iteration the interference powers are set to zero for each θ_{i_m} inside the region $\theta_L(k) \leq \theta \leq \theta_R(k)$.

After finding $d(\theta_{i_m}, k)$ and the beam region, the interference signal powers can be set for the next iteration. Let $\xi_{i_m}(k)$ denote the interference-to-noise ratio (INR) of interference signal m at iteration k. The INRs for iteration $(k+1)$ are set according to

$$\xi_{i_m}(k+1) = \begin{cases} 0 & : \ \theta_{i_m} \in [\theta_L(k), \theta_R(k)] \\ \max[0, \Gamma_{i_m}(k)] & : \ \text{otherwise} \end{cases}, \qquad (12)$$

where

$$\Gamma_{i_m}(k) = \xi_{i_m}(k) + K[p(\theta_{i_m}, k) - d(\theta_{i_m}, k)]. \qquad (13)$$

K is a scalar constant called the *iteration gain.*

The following example shows how a typical pattern evolves during this process. Consider a ten-element array of isotropic elements spaced every half wavelength. Assume the goal is to obtain a weight vector that yields a beam at broadside and uniform sidelobes 30 dB below the peak. All interference powers are initially set to zero and the initial pattern is computed. The result is shown in Figure 13a. It is a standard $[\sin(\frac{N}{2}\sin\theta)]/[\sin(\frac{1}{2}\sin\theta)]$ pattern with 13 dB first sidelobes, where N is the number of elements (10 in this case).

Now we iterate on the interference power. Figure 13b shows the interference spectrum at the first iteration as assigned by 12. In this example $M = 119$ interference signals were used with an iteration gain of $K = 2.0$. Note how the initial interference spectrum mirrors the sidelobes in Fig. 13a.

The first adapted voltage pattern $p(\theta, 1)$ (in response to the interference spectrum of Fig. 13b) is shown in Figure 13c. Also shown in Fig. 13c

(as the dotted line) is the new desired voltage envelope, $d(\theta, 1)$. Note that $d(\theta, 1) < d(\theta, 0)$ because $P(1) < P(0)$ in 11. Figure 13d shows the $k = 2$ interference spectrum, which is noticeably weaker than the $k = 1$ spectrum. Figures 14a,b and c,d show how the algorithm progresses through iterations k =3,4 and k =9,10. Each figure shows the most recent adapted voltage pattern, the desired voltage envelope and the new interference spectrum. Note the evolution of the sidelobes as they approach the desired envelope. Note also the behavior of the beam and the interference spectrum. Eventually, (as long as K is suitably chosen) these figures approach a steady-state where the pattern, spectrum and desired envelope change little from one iteration to the next. The process is stopped when the sidelobe behavior is deemed acceptable or when no further changes occur. As may be seen in the final pattern in Fig. 15, the algorithm performed well for this simple problem.

If the iteration gain K is too large, the algorithm becomes unstable, as one would expect from discrete control theory [21]. The maximum value of K that yields stable operation depends strongly on the desired sidelobe depth $D(\theta)$. The lower the sidelobes, the higher K can be. In practice, suitable values of K are easily found by trial-and-error. To make the algorithm converge as quickly as possible, one wants the largest value of K for which the algorithm is stable.

A typical instability that occurs when K is too large can be seen in the sequence of patterns in Fig. 16. These plots show iterations k=32–35 for the same 10-element array as in Figures 13 and 14. The desired sidelobe level is 35 dB down from the main beam and the gain is purposely set too high at $K = 35.0$. Note that the outer sidelobes (farthest from the beam) oscillate above and below the target level while the inner sidelobes remain

steady.

When this algorithm is applied to an array of *uniformly spaced, isotropic* elements and the goal is to obtain *uniform* sidelobes, the weights obtained converge to the standard Dolph-Chebyshef (DC) weights [17]. For example, Figure 17 compares the patterns obtained with the DC method and our method for a 10-element array with half-wavelength element spacing with the main beam steered to $\theta_d = 25°$ and with the sidelobe level 35 dB down. Figure 17a shows the pattern obtained with the DC method and Fig. 17b shows the pattern from our algorithm after 27 iterations with $K = 25$. As may be seen, the patterns in Figures 17a and b are virtually identical. Comparison of the weight vectors obtained with the two methods shows that the weights obtained with our algorithm converge to the Dolph-Chebyshef weights [9].

However, the Dolph-Chebyshef method is applicable only to arrays for which the elements are uniformly spaced and isotropic. The advantage of our adaptive array algorithm, is that it can handle arbitrary element patterns and spacings. The element patterns and spacings are included in the procedure from the beginning.

As an example of an array with nonisotropic elements, consider an array of 30 short dipoles in which the dipoles are aligned with the array axis and spaced every half wavelength. Assume the pattern of every element is $f_j(\theta) = \cos\theta$. Suppose the goal is a beam steered to $\theta_d = 45°$ with uniform sidelobes 35 dB down. The only way the DC method can be used with such a set of elements is to calculate the DC weights for a 30-element array of isotropic elements and then simply use these weights with the nonisotropic elements. For example, Figure 18 shows the pattern that results if DC weights are used with isotropic elements. When the DC weights are used

with the *dipole* array, the resulting pattern is shown in Fig. 19a. Note that the sidelobes in Fig. 19a are no longer uniform but are tapered by the element pattern. Note also that the sidelobe level at $\theta = 0°$ is *not* 35 dB below the beam peak as desired.

However, if the adaptive array algorithm is used with the dipole array, the final pattern obtained is shown in Figure 19b. Note how much closer the sidelobes come to meeting the original uniform design objective when the adaptive array algorithm is used.

As mentioned above, the iterative algorithm can also handle arbitrary element spacings. The problem of designing an array for low sidelobes with arbitrary element spacing has no solution in the literature.

As an example of this type of problem, consider a 33-element linear array of dipoles with nonuniform spacing and orientation. Let the element pattern for dipole j be given by

$$f_j(\theta) = \frac{\cos[\pi l_j \sin(\theta + \tau_j)] + \cos(\pi l_j)}{\cos(\theta + \tau_j)}, \tag{14}$$

where l_j is the dipole length in wavelengths, τ_j is the dipole tilt angle from the array axis, and θ is the angle of an incoming signal measured from the broadside direction to the array axis. Suppose the dipoles in the array vary in length, tilt angle and spacing. For the examples below, we used the (arbitrary) set of array parameters shown in Table 1. We show two cases here. For the first case, the goal is to achieve 30 dB uniform sidelobes with the beam steered to $\theta_d = 0°$. Fig. 20a shows the initial pattern and Fig. 20b shows the final pattern after 5 iterations with $K = 1.0$ for iterations 1 and 2 and $K = 0.5$ for iterations 3-5. Note the improvement in the sidelobes. For the second case, the goal is to achieve 40 dB uniform sidelobes with this array. In this case the final pattern is shown in Fig. 20c. Note that for this case the sidelobes do not meet the 40 dB specification. It turns out

Table 1: Parameters for the 33-element linear array. l_j and d_j are in wavelengths, τ_j is in degrees.

j	l_j	τ_j	d_j	j	l_j	τ_j	d_j
1	0.25	0.0	0.5	18	0.25	0.0	0.50
2	0.25	0.5	0.5	19	0.24	5.0	0.45
3	0.24	5.0	0.55	20	0.26	4.7	0.55
4	0.20	-32.	0.54	21	0.27	-8.9	0.54
5	0.26	-3.2	0.60	22	0.28	3.0	0.53
6	0.27	10.	0.45	23	0.25	3.2	0.56
7	0.23	1.0	0.46	24	0.25	2.8	0.54
8	0.24	0.0	0.50	25	0.25	2.9	0.56
9	0.25	0.0	0.50	26	0.23	1.5	0.50
10	0.21	7.0	0.51	27	0.27	0.7	0.50
11	0.28	6.0	0.47	28	0.28	0.33	0.50
12	0.30	4.4	0.48	29	0.24	0.0	0.57
13	0.29	0.0	0.61	30	0.24	0.43	0.51
14	0.19	1.0	0.57	31	0.25	-20.	0.52
15	0.22	-2.1	0.65	32	0.26	0.8	0.49
16	0.22	3.0	0.42	33	0.25	-9.6	–
17	0.25	0.0	0.50				

that these are the best sidelobes that could be achieved with this array.

This example illustrates the fact that it is not necessarily possible to meet an arbitrary pattern specification with a given set of elements. When the design objective is unattainable with the given array, one finds that the algorithm settles into a steady-state pattern that, while not meeting the objectives, is essentially the best that can be achieved. When the objective is attainable, the algorithm finds a suitable solution quickly.

The algorithm can also be used to produce patterns in which the desired sidelobe level $D(\theta)$ varies as a function of θ. We give two examples below.

First, suppose a pattern is desired whose sidelobes meet the design envelope shown in Fig. 21. The segment of $D(\theta)$ to the left of the beam

slopes at 0.20 dB/degree, meeting the $\theta_d = 10°$ axis at 30 dB below the beam peak. The segment to the right of the beam is flat at 30 dB below the peak. If the algorithm is applied to an array of 17 half-wavelength spaced, isotropic elements, the final pattern is shown in Figure 21b. 25 iterations of the algorithm were performed. The iteration gain K was set to $K = 2.0$ for iterations 1-9 and reduced to $K = 1.2$ for iterations 10-25. The final pattern clearly meets the objective.

Next, suppose the objective is to achieve the sidelobe behavior shown in Fig. 22a. This $D(\theta)$ has three flat segments: 40 dB below the peak for $-90° < \theta \leq -42°$, 30 dB below the peak for $-42° < \theta \leq 42°$, and 40 dB below the peak for $42° < \theta < 90°$. The beam is at $\theta_d = 0°$. For this example, we use an array of 24 center-excited quarter-wavelength dipoles. The dipoles have their axes aligned with the array axis and have a uniform half wavelength center-to-center spacing. Figure 22b shows the result of using the algorithm on this array with the $d(\theta)$ in Fig. 22a. The iteration gain was $K = 1.5$ for iterations 1-14, $K = 1.0$ for iterations 15-22, and $K = 0.7$ for iterations 23-29.

The examples above illustrate the usefulness of this algorithm. It can handle arrays with nonuniformly spaced elements and with nonisotropic and unequal element patterns, and it can also handle problems where the desired sidelobe level varies with angle.

5. Element reuse in adaptive arrays

The final area of research under JSEP involved the issue of element *reuse* in adaptive arrays. The purpose of this effort was to determine whether it is feasible to use the same elements of a phased array to form both the main beam and one or more auxiliaries for use in a sidelobe canceller array. We have submitted a paper [22] to the IEEE Transactions on Antennas and

Propagation based on this work.

A sidelobe canceller (SLC) is an adaptive antenna system that uses a main antenna with a large aperture and one or more auxiliary antennas [2,20]. An adaptive processor combines the signals from these antennas so that interfering signals in the sidelobe region of the main antenna are suppressed.

The performance of conventional SLCs that use separate main and auxiliary antennas is well known [2,20]. These arrays perform best when the main antenna has a low sidelobe level and the auxiliary antennas have patterns with maxima near the interfering signal arrival angles. The difference between a conventional SLC and a sidelobe canceller with element reuse is that the noise components in the mainbeam and auxiliary signals are correlated. Because the weights in a SLC attempt to cancel all components in the main channel that are correlated with the auxiliary signals, this noise correlation affects array performance. It turns out that the most important effect of element reuse is that the sidelobe level (SLL) of the adapted pattern can be seriously degraded. In particular, whenever the number of adaptive degrees of freedom exceeds the number needed to suppress the interference, large SLL increases may result. This effect is undesirable in radar applications where the mainbeam pattern is designed for low sidelobes and retention of these low sidelobes is essential to avoid clutter degradation.

For example, consider a 100 element array of isotropic elements in which the mainbeam pattern is formed from all 100 elements. Suppose a 55 dB Dolph-Chebyshef amplitude taper is used, with the beam steered to 30° from broadside, and let the Chebyshef weights be randomized slightly to make the pattern more realistic. A typical pattern that results is shown in Figure 23. Suppose a single element, element 50 near the center of the array,

is then used to form an auxiliary signal as well. (It was also used to form the mainbeam.) For the case where the desired signal arrives from 30° (the mainbeam direction), a single jammer arrive from $\theta_i = -45°$, the desired signal-to-noise ratio (SNR) per element is -30 dB, and the interference-to-noise ratio (INR) per element is 40 dB, the adapted pattern is shown in Figure 24. The jammer null is evident at $-45°$. The SLL of this adapted pattern is only slightly higher than that of the mainbeam pattern.

But now consider what happens if this canceller operates with *no* jammer incident. The adapted pattern for this case is shown in Figure 25. The sidelobes are now much higher than those of the mainbeam pattern. The average increase SLL increase turns out to be 22.7 dB in this case. The reason for this sidelobe degradation is that the noise components in the main beam and in the auxiliary are correlated, due to the element reuse. Because the noise in the auxiliary is also present in the main beam, the adaptive canceller minimizes the output noise power by setting the auxiliary weight equal to the negative of the mainbeam combiner weight on that element. As a result, the net weight on the element used for the auxiliary is zero. The adapted pattern is the same as the pattern the mainbeam would have if the auxiliary element were removed. The high sidelobe response in Figure 25 is typical of what happens when a center element is removed from a Chebyshef taper.

This problem may be avoided by using for each auxiliary a combination of array elements such that the set of weights used to form the auxiliary signal are orthogonal to the set used to form the main beam signal. If this is done, the sidelobes will remain low when the number of auxiliaries exceeds the number of jammers.

For example, consider a sidelobe canceller using the main beam pattern

in Figure 23 with two auxiliary signals, one formed from elements 49 and 50, and the other from elements 51 and 52. Suppose the auxiliary weights for the pair of elements in each auxiliary are chosen to be orthogonal to the mainbeam combiner weights. Figure 26 shows the average increase in SLL that results with this combination for a single 40 dB CW jammer as a function of its arrival angle θ_{i_1}. Auxiliaries chosen to be orthogonal to the main beam yield much better SLL performance.

References

[1] Joint Services Electronics Program Eleventh Annual Report, Report No. 720440-1, November 1988, The ElectroScience Laboratory, Department of Electrical Engineering, The Ohio State University, Columbus, OH 43212; prepared under Contract N00014-88-K-0004 for the Department of the Navy, Office of Naval Research, 800 North Quincy Street, Arlington, VA 22217.

[2] R. T. Compton, Jr., *Adaptive Antennas: Concepts and Performance*, Prentice-Hall, Inc., Englewood Cliffs, NJ, 1988.

[3] R. T. Compton, Jr., "The Bandwidth Performance of a Two-Element Adaptive Array with Tapped Delay-Line Processing," *IEEE Transactions on Antennas and Propagation*, AP-36, 1 (January 1988), p.5.

[4] R. T. Compton, Jr., "The Relationship Between Tapped Delay-Line and FFT Processing in Adaptive Arrays," *IEEE Transactions on Antennas and Propagation*, AP-36, 1 (January 1988), p.15.

[5] Frederick Vook, "The Bandwidth Performance of Adaptive Arrays with Tapped Delay-Line Processing," M. Sc. Thesis, March 1989, Department of Electrical Engineering, The Ohio State University, Columbus, OH.

[6] F. Vook and R. T. Compton, Jr., "The Bandwidth Performance of Linear Adaptive Arrays with Tapped Delay-Line Processing," submitted for publication to *IEEE Transactions on Antennas and Propagation.*

[7] L. Kleinrock and F. A. Tobagi, "Packet Switching in Radio Channels: Part I - Carrier Sense Multiple Access Modes and Their Throughput-Delay Characteristics," *IEEE Transactions on Communications*, COM-23, 12 (December 1975), p.1400.

[8] Carl A. Olen, "A Sidelobe Control Algorithm Using Adaptive Array Techniques," M. Sc. Thesis, August 1989, Department of Electrical Engineering, The Ohio State University, Columbus, OH.

[9] Carl A. Olen and R. T. Compton, Jr., "A Numerical Pattern Synthesis Algorithm for Arrays," submitted to *IEEE Transactions on Antennas and Propagation.*

[10] T. T. Taylor, "Design of Line Source Antennas for Narrow Beamwidth and Low Sidelobes," *IRE Transactions on Antennas and Propagation*, AP-3, 1955, p.16.

[11] R. F. Hyneman and R. M. Johnson, "A Technique for the Synthesis of Shaped-Beam Radiation Patterns with Approximately Equal-Percentage Ripple," *IEEE Transactions on Antennas and Propagation*, AP-15, 1967, p. 736.

[12] R. F. Hyneman, "A Technique for the Synthesis of Line-Source Antenna Patterns Having Specified Sidelobe Behavior," *IEEE Transactions on Antennas and Propagation*, AP-16, 1968, p. 430.

[13] R. S. Elliott, "Design of Line Source Antennas for Narrow Beamwidth and Asymmetric Low Sidelobes," *IEEE Transactions on Antennas and Propagation*, AP-23, 1975, p.100.

[14] R. S. Elliott, "Design of Line Source Antennas for Sum Patterns with Sidelobes of Individually Arbitrary Heights," *IEEE Transactions on Antennas and Propagation*, AP-24, 1976, p.76.

[15] R. S. Elliott, "Design of Line Source Antennas for Difference Patterns with Sidelobes of Individually Arbitrary Heights," *IEEE Transactions on Antennas and Propagation*, AP-24, 1976, p. 310.

[16] W. D. White, "A Flexible Synthesis Procedure for Line Source Antennas," *IEEE Transactions on Antennas and Propagation*, AP-24, 1976, p.857.

[17] C. L. Dolph, "A Current Distribution for Broadside Arrays which Optimizes the Relationship between Beamwidth and Sidelobes," *Proceedings of the IRE*, vol. 34, 1946, p.335.

[18] A. T. Villeneuve, "Taylor Patterns for Discrete Arrays," *IEEE Transactions on Antennas and Propagation*, AP-32, 1984, p.1089.

[19] R. S. Elliott and G. J. Stern, "A New Technique for Shaped Beam Synthesis of Equispaced Arrays," *IEEE Transactions on Antennas and Propagation*, AP-32, 1984, p.1129.

[20] S. P. Applebaum, "Adaptive Arrays," *IEEE Transactions on Antennas and Propagation*, AP-24, 1976, p.585.

[21] K. Ogata, *Discrete-Time Control Systems*, Englewood Cliffs, N.J., Prentice-Hall, 1987.

[22] J. Ward and R. T. Compton, Jr., "Sidelobe Level Performance of Adaptive Sidelobe Canceller Arrays with Element Reuse," submitted to *IEEE Transactions on Antennas and Propagation.*

6. List of Papers - JSEP Adaptive Array Studies

Published:

1. M.W. Ganz and R.T. Compton, Jr. "A Data-Derived Reference Signal Technique for Adaptive Arrays," *IEEE Transactions on Communications*, Vol. 37, No. 9, pp. 975-983, September 1989.

Submitted for Publication:

1. F.W. Vook and R.T. Compton, Jr. "The Bandwidth Performance of Adaptive Arrays with Tapped Delay-Line Processing," *IEEE Transactions on Antennas and Propagation.*

2. C.A. Olen and R.T. Compton, Jr. "A Numerical Pattern Synthesis Algorithm for Arrays," *IEEE Transactions on Antennas and Propagation.*

Papers in Preparation:

1. J.W. Ward and R.T. Compton, Jr. "Sidelobe Level Performance of Adaptive Sidelobe Canceller Arrays with Element Reuse."

2. R.T. Compton, Jr. "Adaptive Arrays in Packet Radio Systems."

Conferences/Oral presentations:

1. J.W. Ward and R.T. Compton, Jr. , "Adaptive Arrays in Packet Radio," 1989 Communication Theory Workshop, Hawks Cay, Florida, April 9-12, 1989.

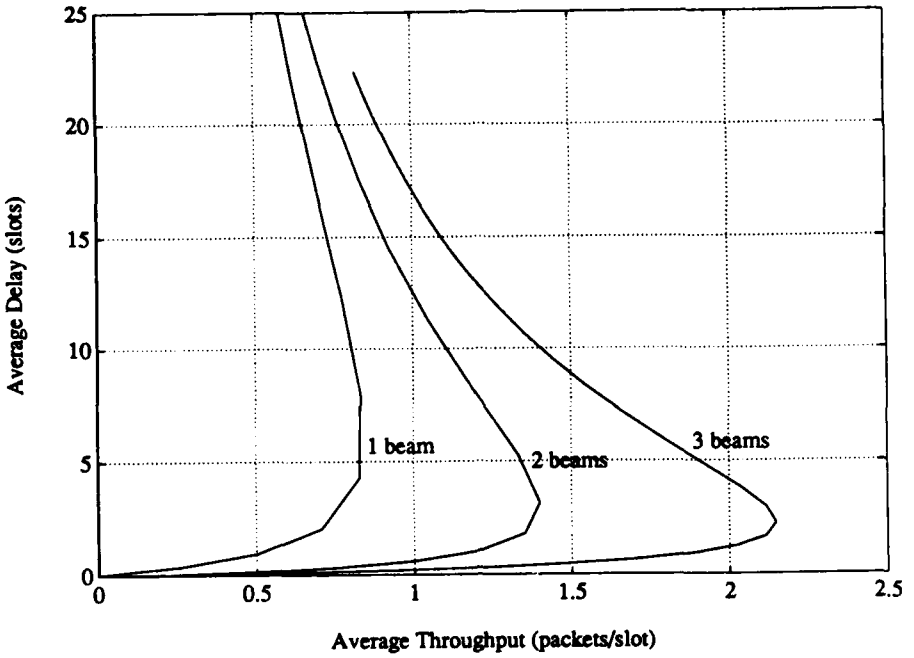

Figure 9: Delay versus Throughput ($N = 16$, $\theta_r = 10°$, $T_u = 61$ bits)

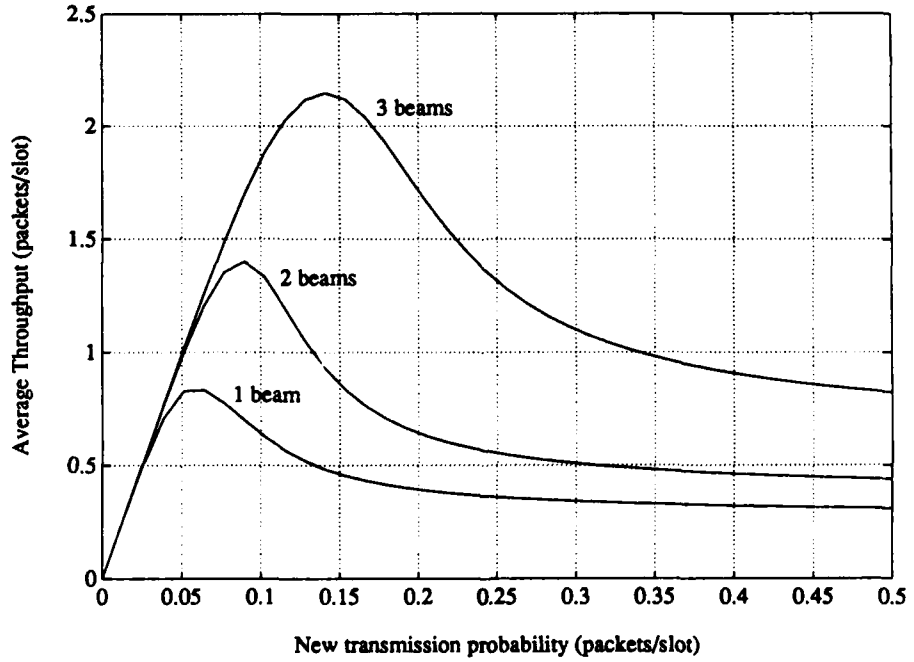

Figure 10: Throughput versus New Transmission Probability ($N = 16$, $\theta_r = 10°$, $T_u = 61$ bits)

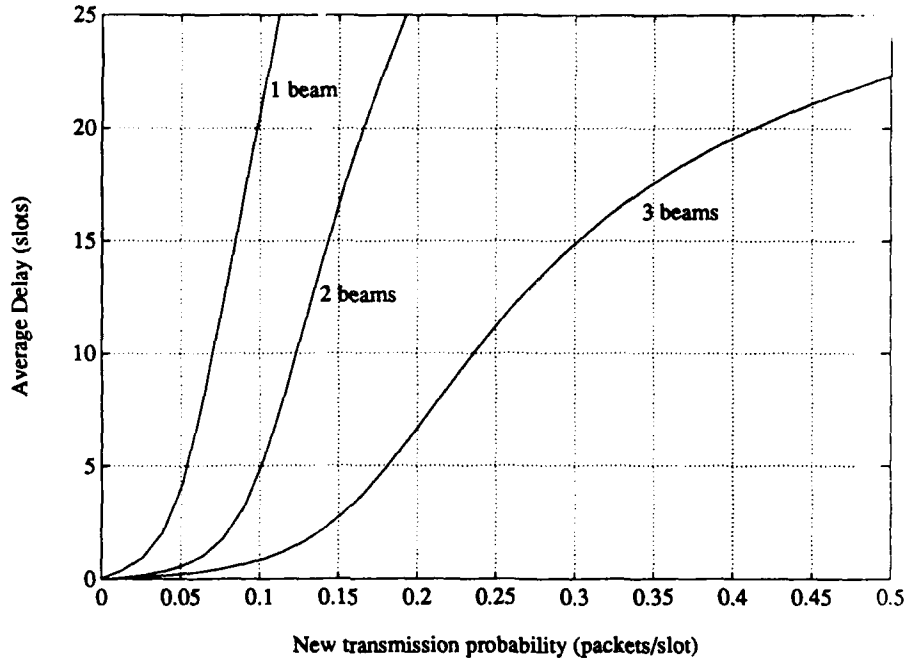

Figure 11: Delay versus New Transmission Probability ($N = 16$, $\theta_r = 10°$, $T_u = 61$ bits)

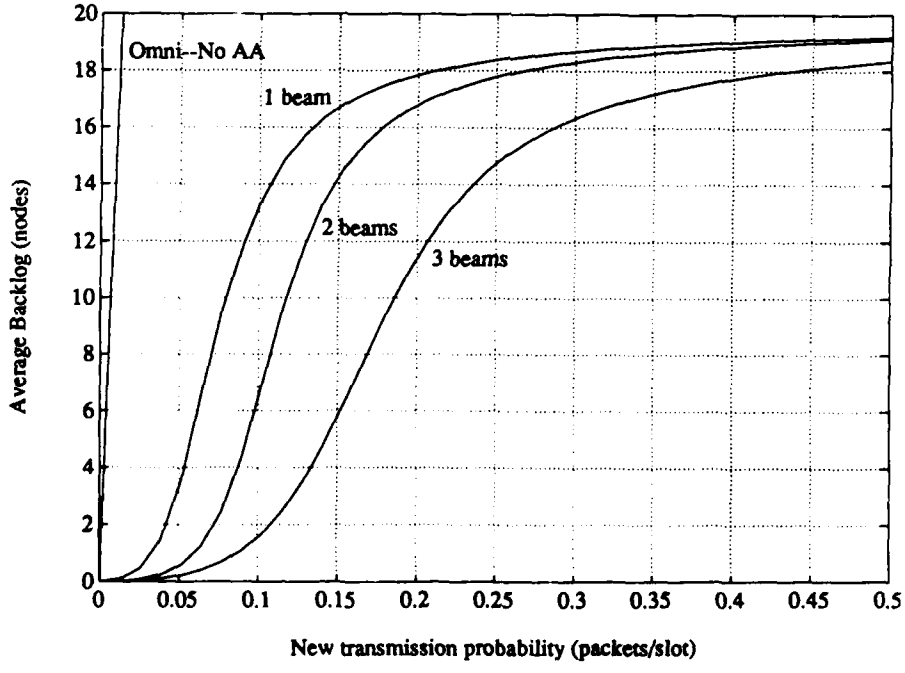

Figure 12: Backlog versus New Transmission Probability ($N = 16$, $\theta_r = 10°$, $T_u = 61$ bits)

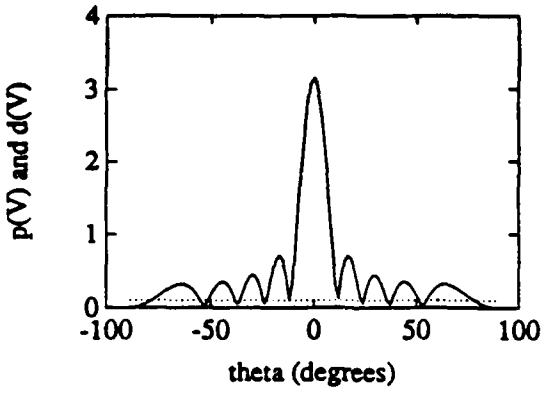

a. $p(\theta, 0)$ and $d(0)$

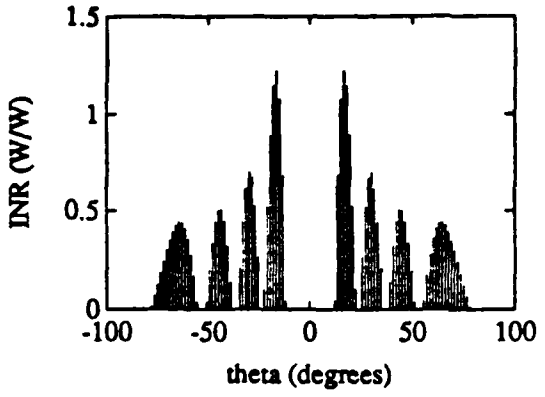

b. Interference spectrum: $k = 1$

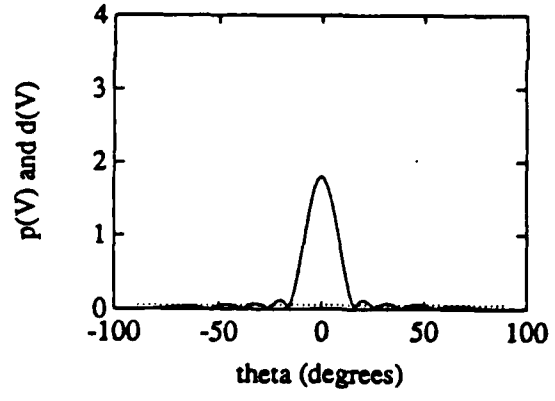

c. $p(\theta, 1)$ and $d(1)$

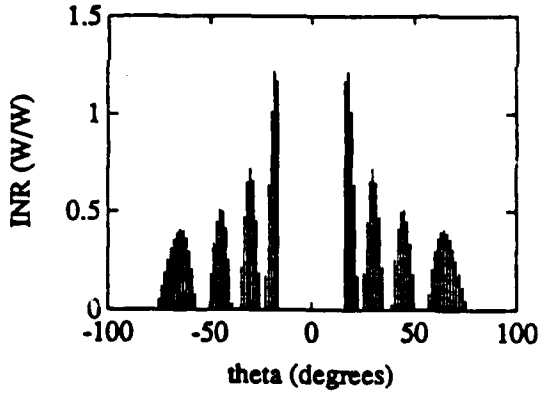

d. Interference spectrum: $k = 2$

Figure 13: Patterns and interference powers. (The dotted line is $d(\theta, k)$.)

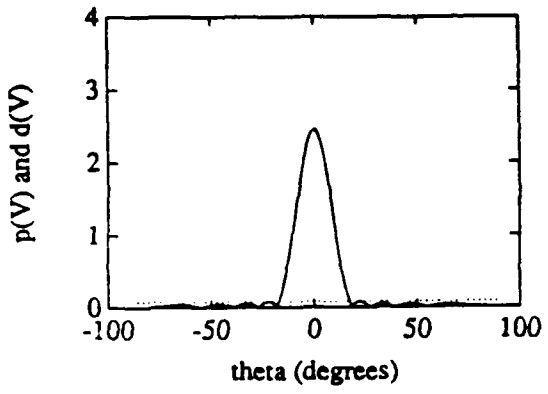

a. $p(\theta, 3)$ and $d(3)$

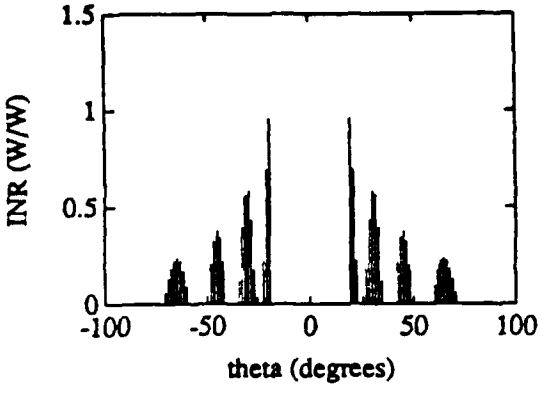

b. Interference spectrum: $k = 4$

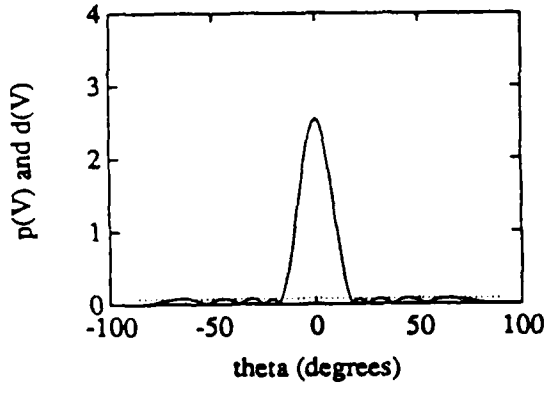

c. $p(\theta, 9)$ and $d(9)$

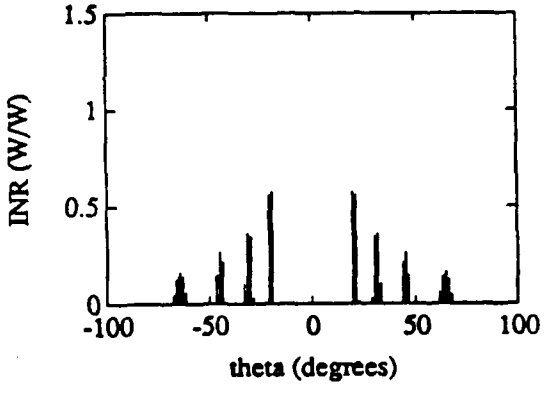

d. Interference spectrum: $k = 10$

Figure 14: Patterns and interference powers. (The dotted line is $d(\theta, k)$.)

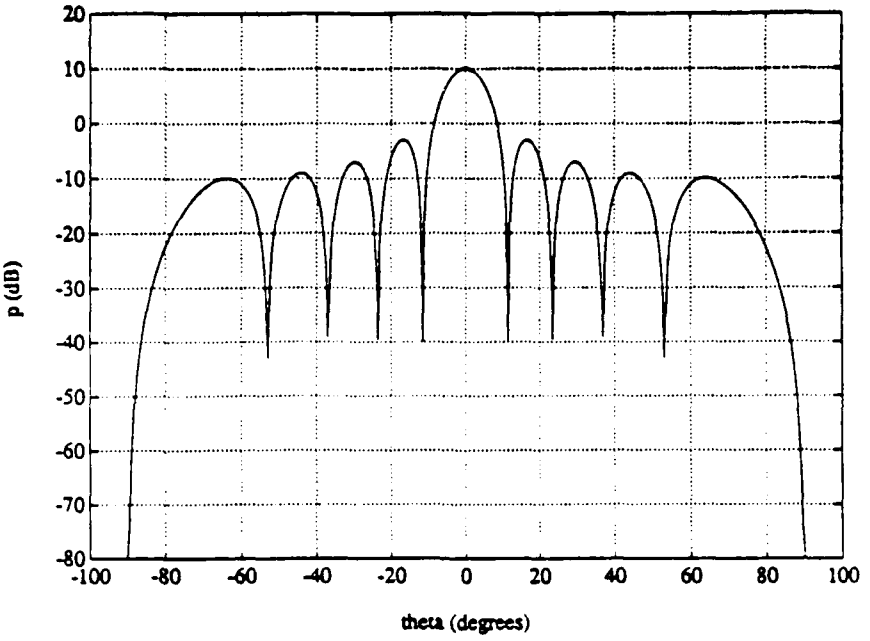

a. Initial Pattern

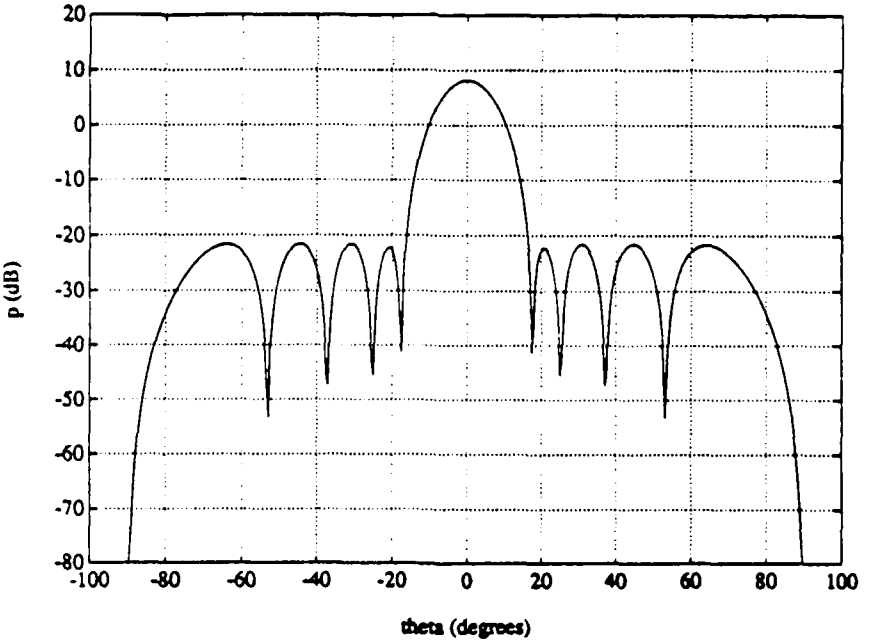

b. Final Pattern

Figure 15: Initial and final patterns: 10-element array, isotropic elements

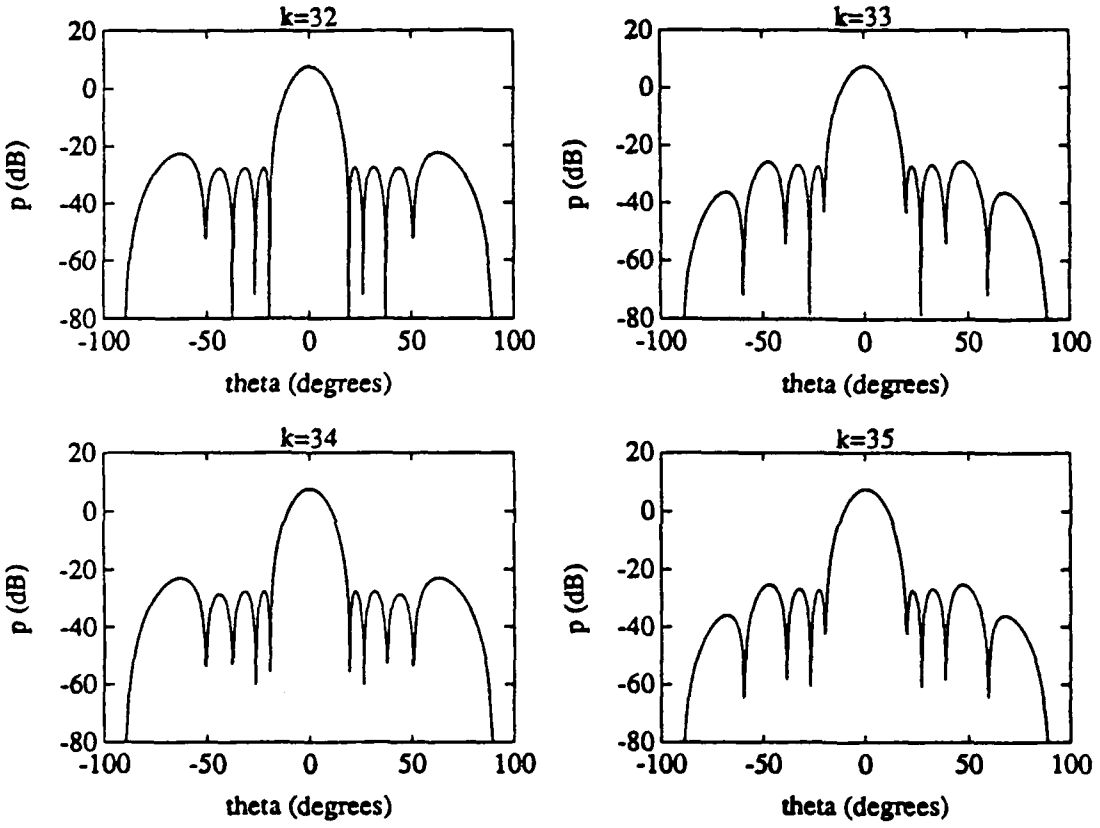

Figure 16: An example of instability

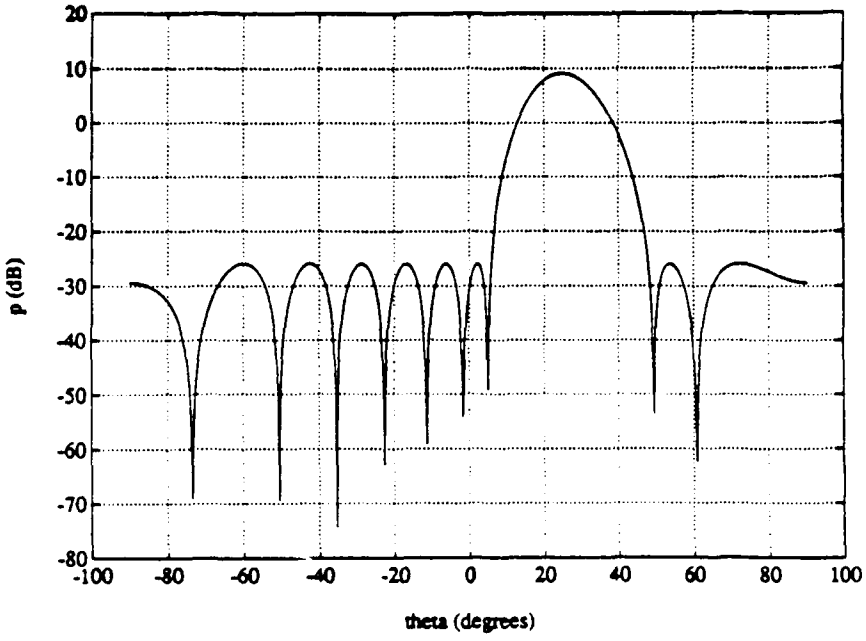

a. Dolph-Chebyshef pattern

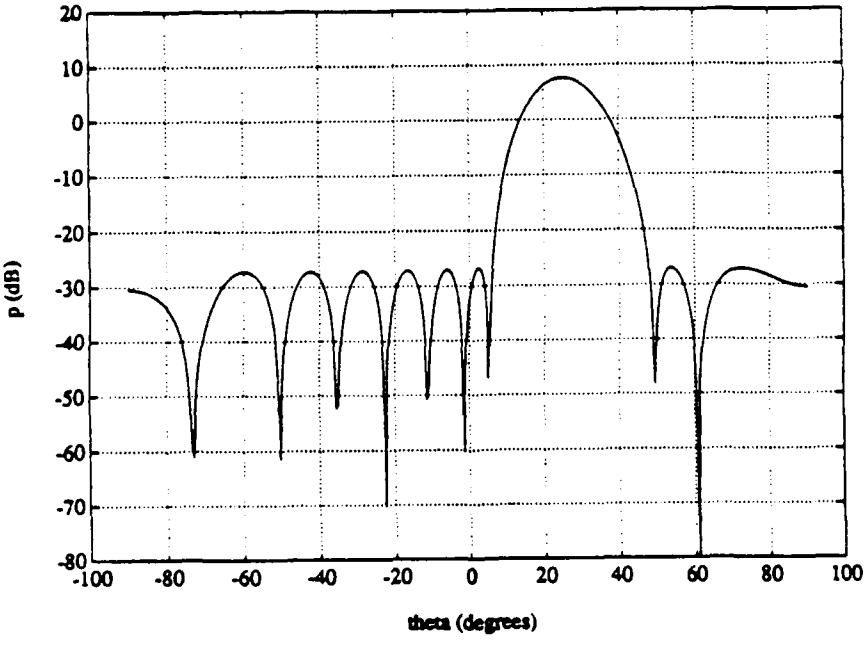

b. Pattern obtained with the adaptive algorithm

Figure 17: Patterns: 10 isotropic elements, half-wavelength spacing

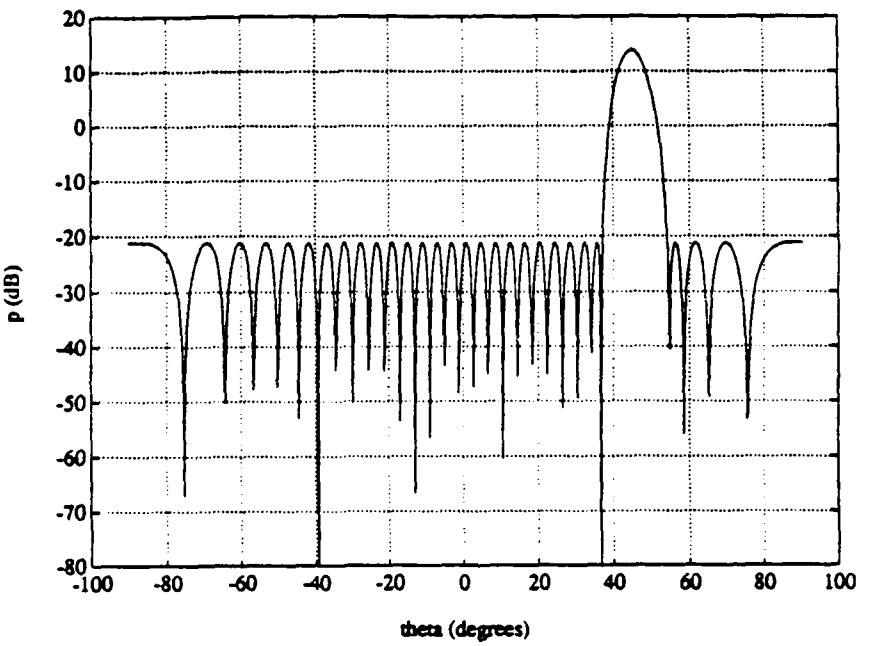

Figure 18: Dolph-Chebyshef pattern of a 30 element array: isotropic elements, half-wavelength spacing, $\theta_d = 45°$.

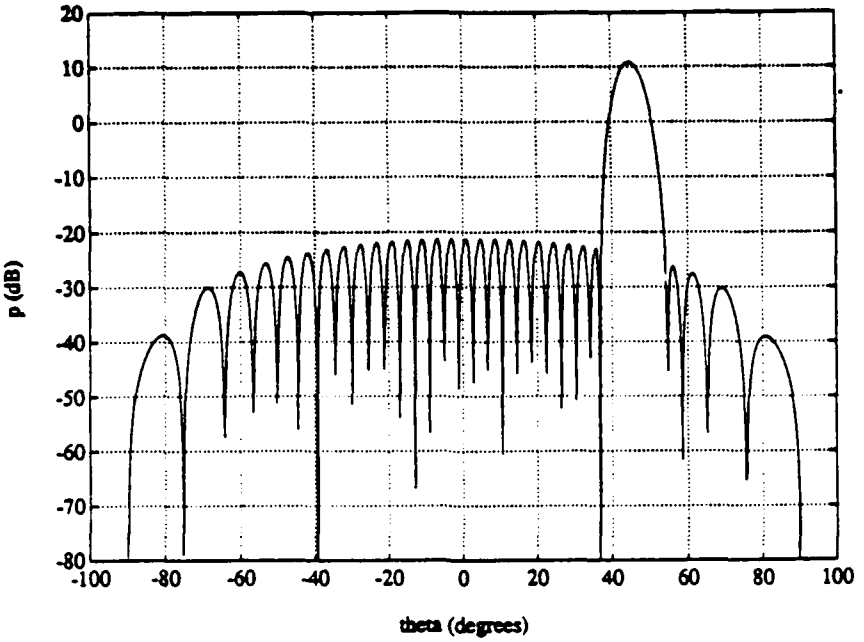

a. Dolph-Chebyshef weights

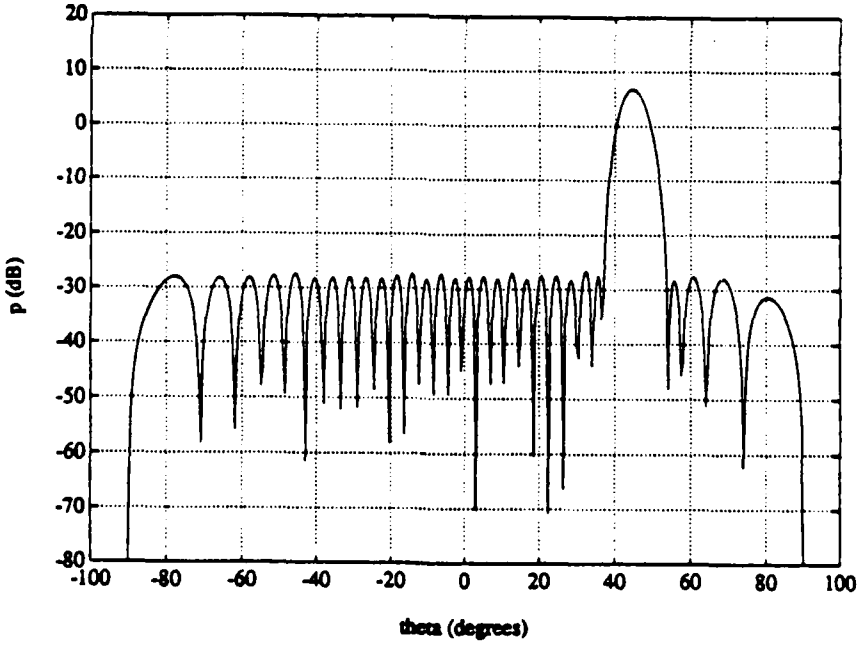

b. Weights obtained from the adaptive array algorithm

Figure 19: Patterns for 30 short dipoles, $\theta_d = 45°$

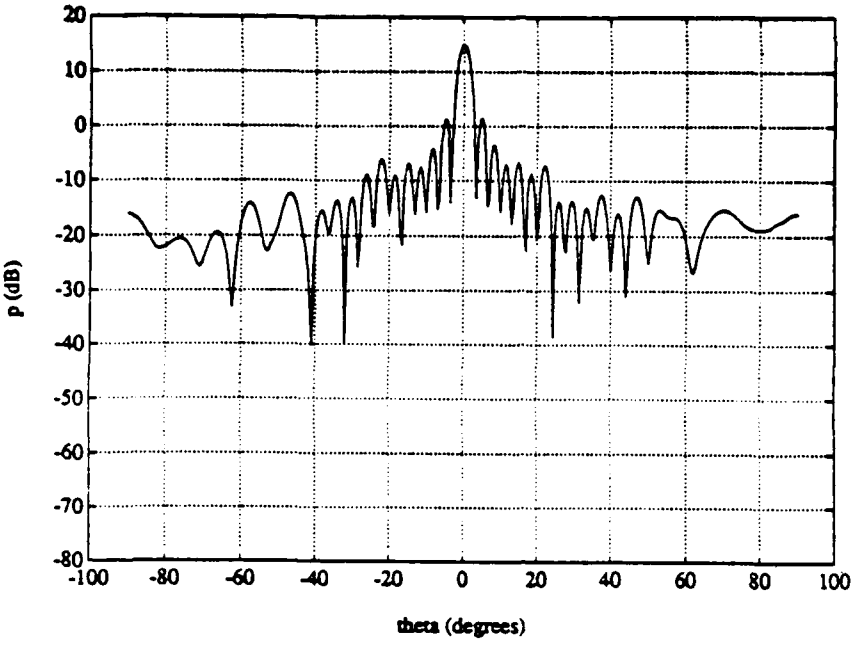

a. Initial pattern

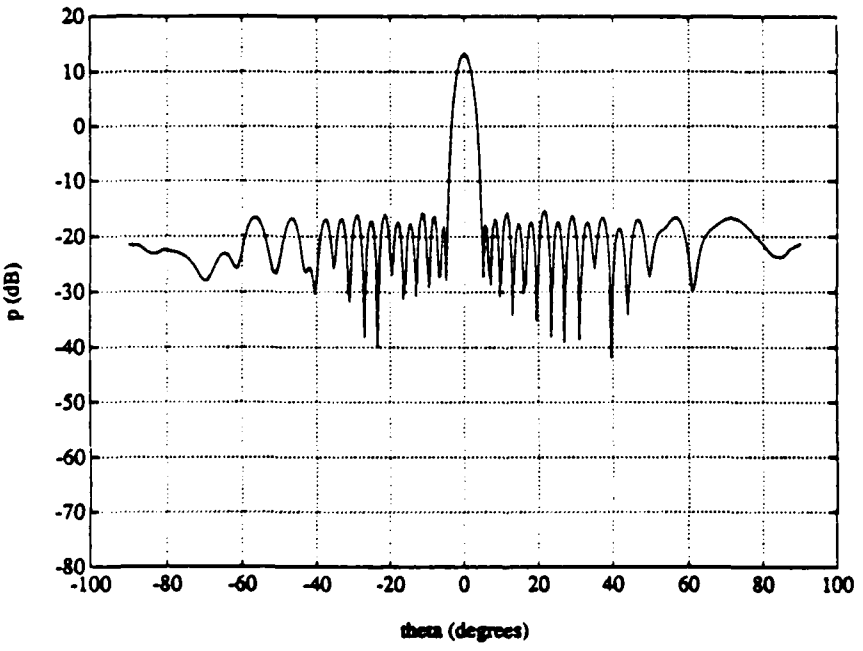

b. Final pattern: 30 dB sidelobe design

Figure 20: Patterns for the array of Table 1.

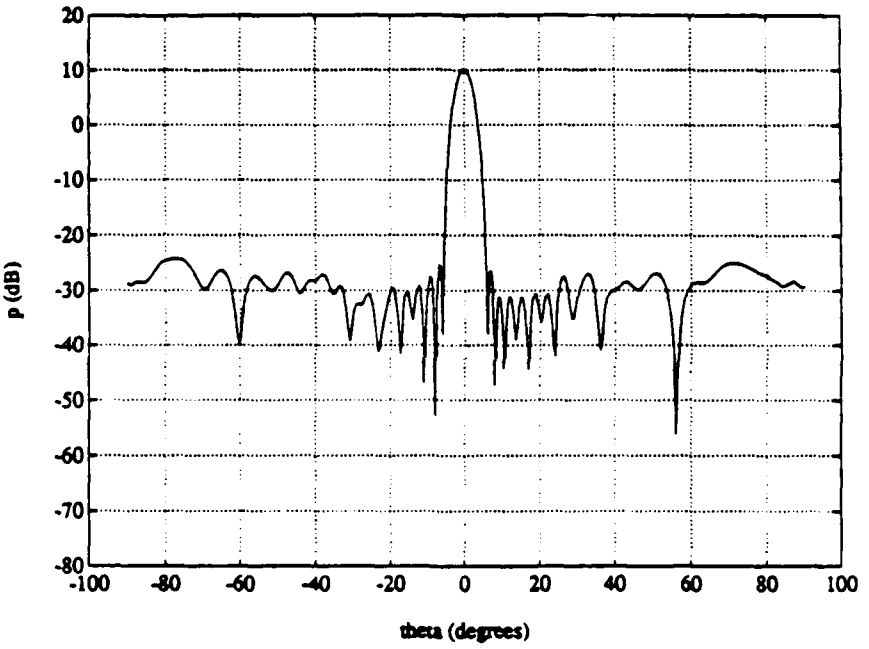

c. Final pattern: 40 dB sidelobe design

Figure 20: Patterns for the array of Table 1.

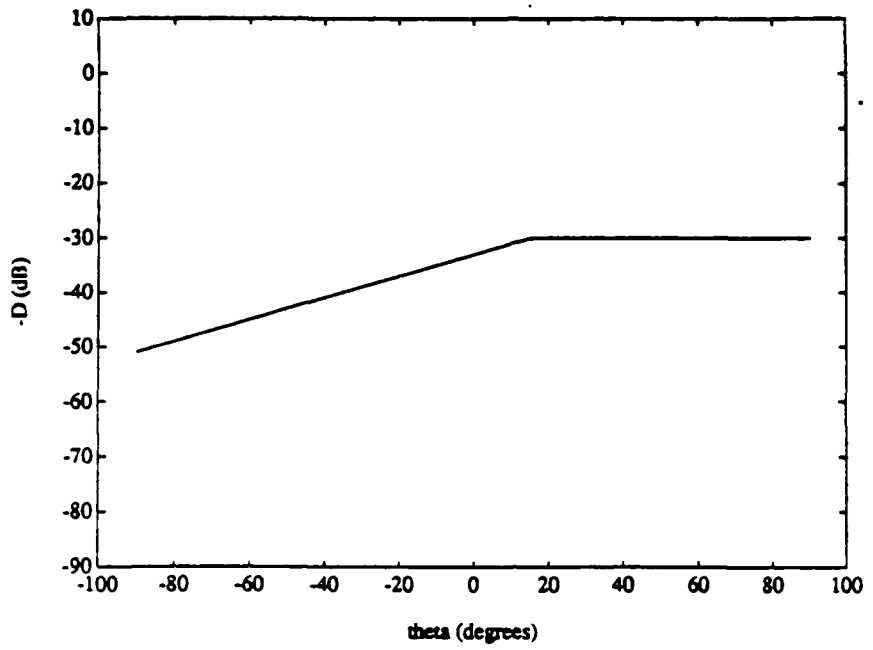

a. Desired envelope function

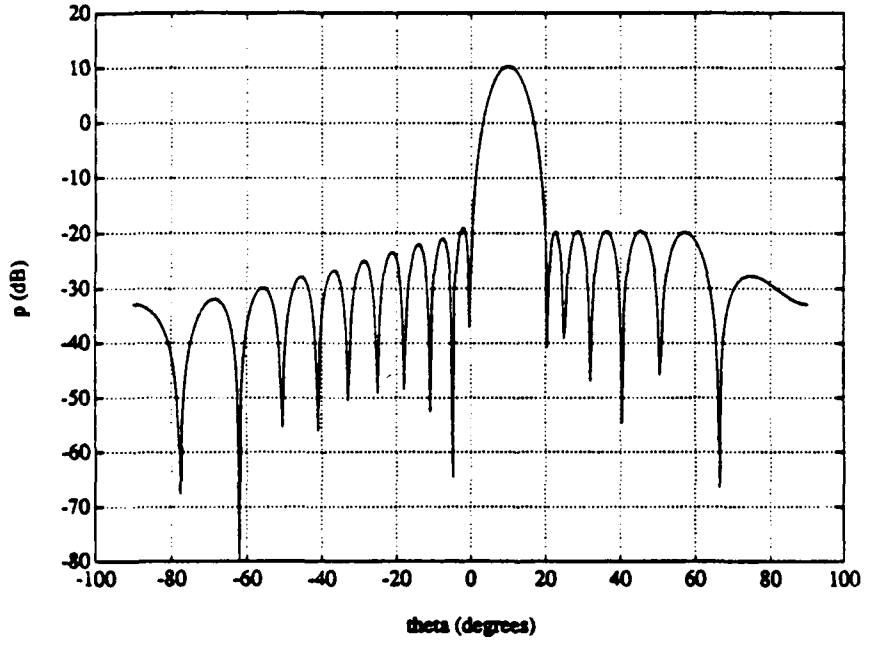

b. Shaped pattern

Figure 21: A two-segment nonuniform sidelobe problem

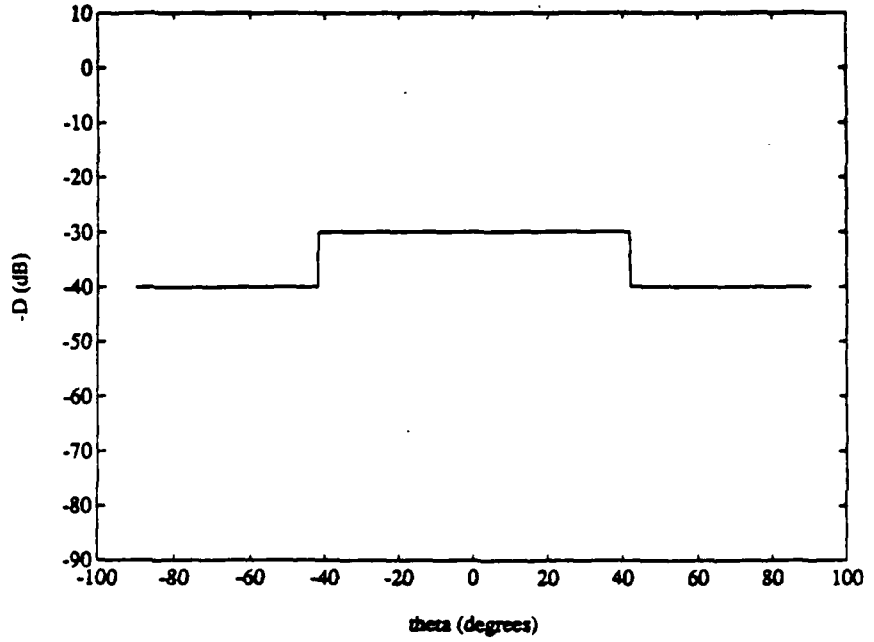

a. Desired envelope function

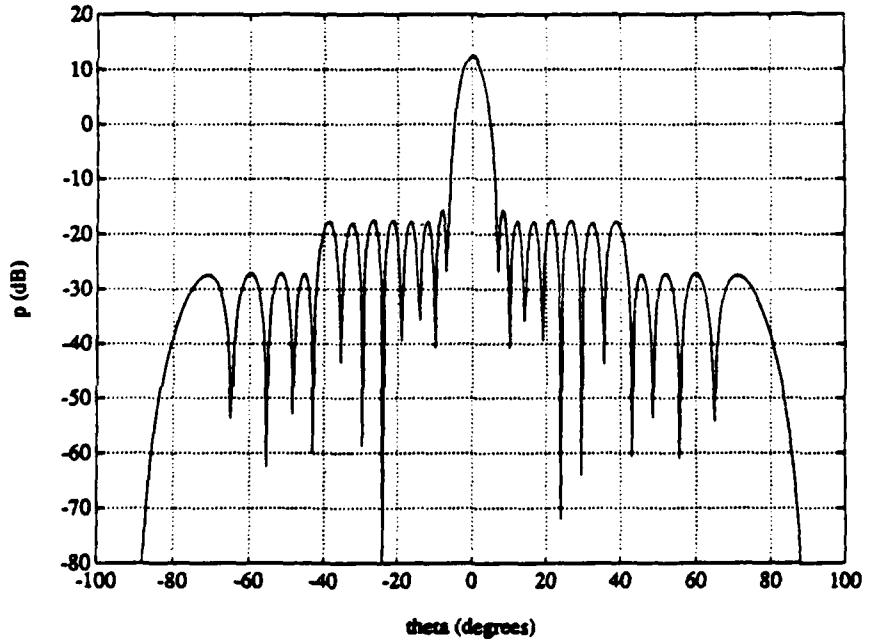

b. Shaped pattern

Figure 22: A three-segment nonuniform sidelobe problem

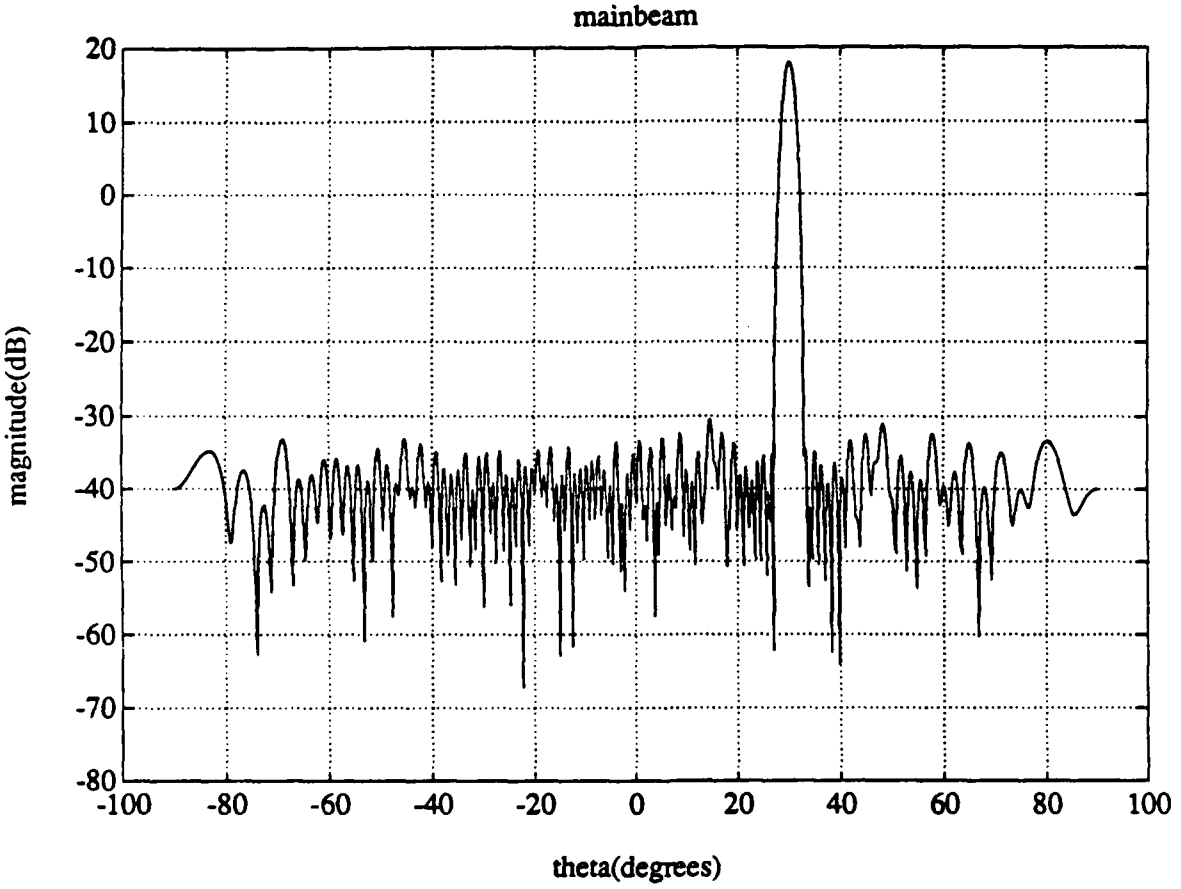

Figure 23: The mainbeam pattern of a 100 element array with 55 dB Dolph-Chebyshev weights and a beam angle of $\theta_d = 30°$

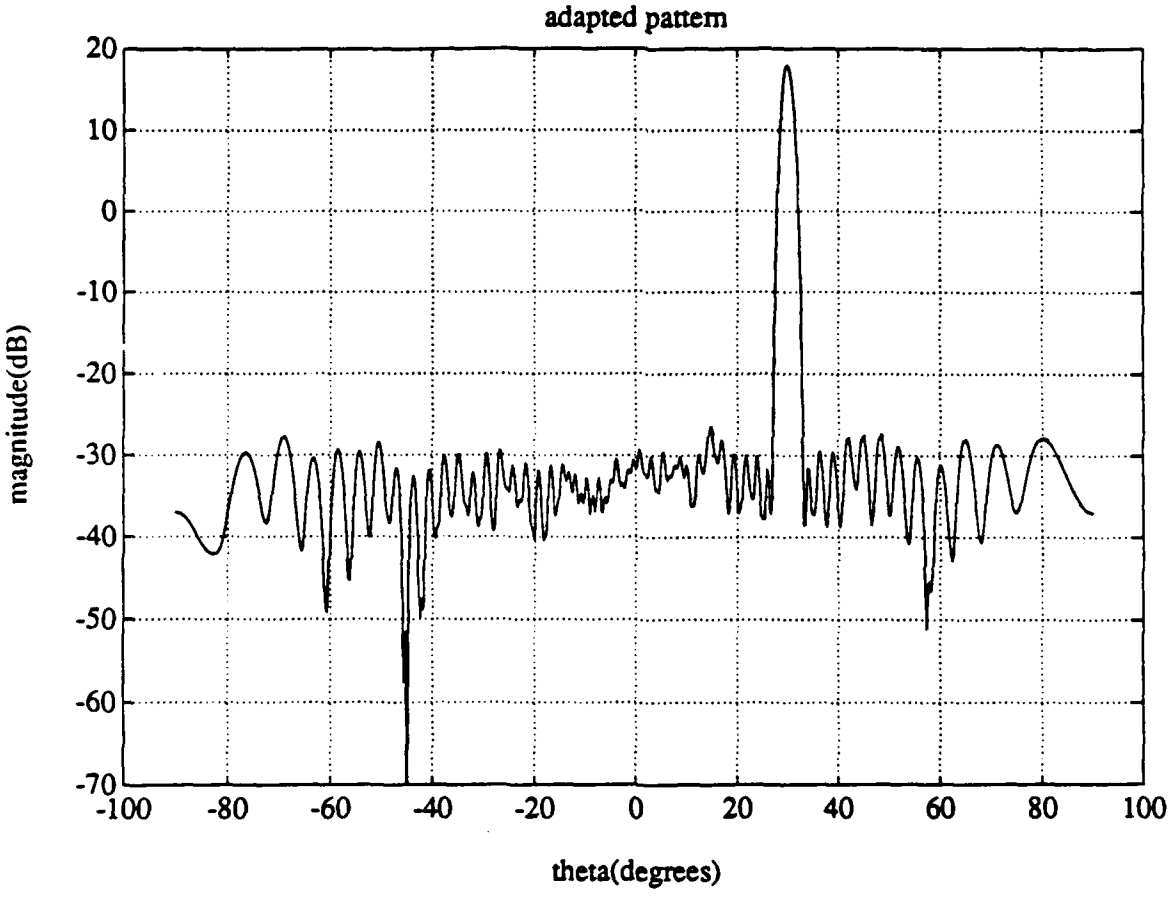

Figure 24: Adapted pattern for a SLC using element 50 as the auxiliary element. One 40 dB CW jammer, at $\theta_{i_1} = -45°$. SNR=-30dB, $\theta_d = 30°$.

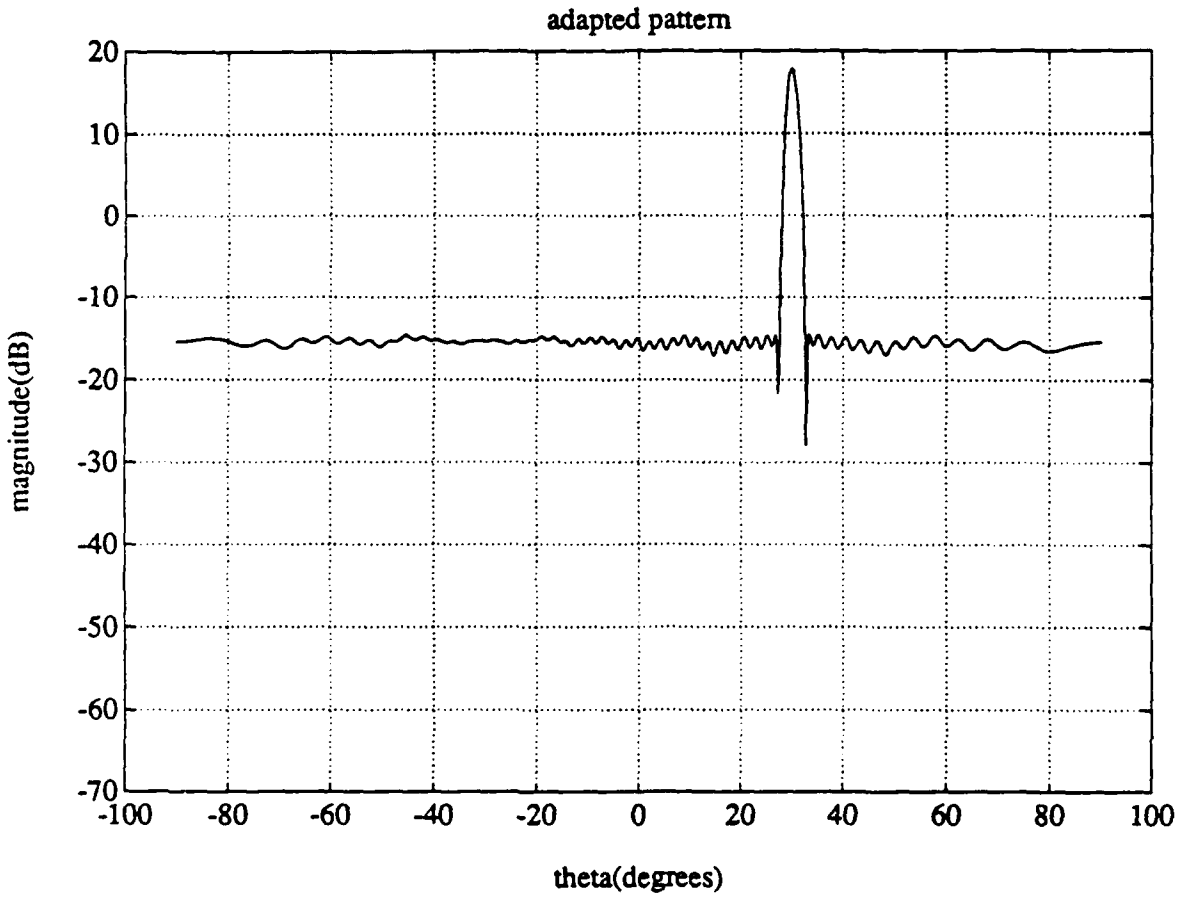

Figure 25: Adapted pattern for a SLC using element 50 as the auxiliary element. No jammers present. SNR=-30dB, $\theta_d = 30°$.

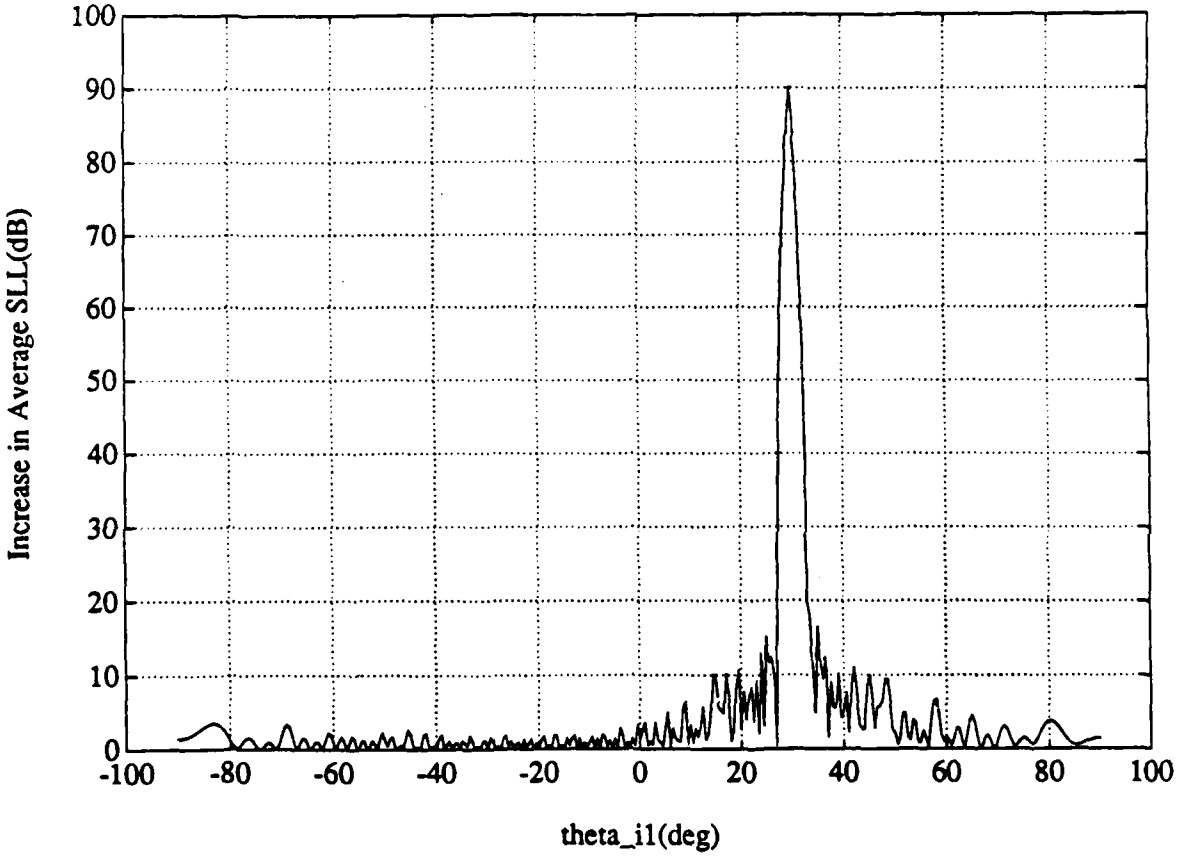

Figure 26: SLL increase for a canceller using two auxiliaries: elements 49-50 and 50-51. A single 40 dB CW jammer is incident from θ_{i_1}.